Efficient Spintronic Terahertz Emitters: Basic principles and technical realization

René Beigang
Rheinland-Pfälzische Technische Universität RPTU
Kaiserslautern - Landau
Germany

Efficient spintronic terahertz emitters:
Basic principles and technical realization

René Beigang

Rheinland-Pfälzische Technische Universität RPTU
Kaiserslautern - Landau
Germany

The Abdus Salam
International Centre
for Theoretical Physics

Trieste
6.2.2023

Efficient spintronic terahertz emitters:
Basic principles and technical realization

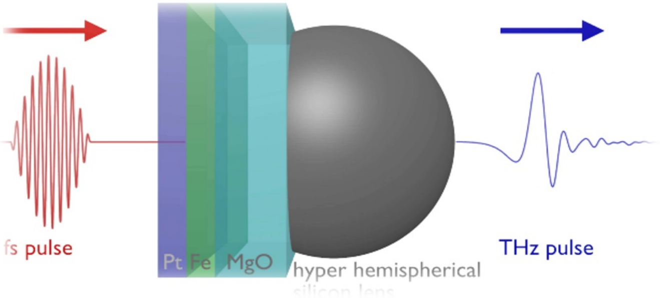

René Beigang
Rheinland-Pfälzische Technische Universität RPTU
Kaiserslautern - Landau
Germany

Laura Scheuer
Garik Torosyan → Photonic Center Kaiserslautern
Evangelos Papaioannou → University of Halle

Valynn K. Mag-usara
Jessica Afalla
Masahiko Tani → University of Fukui, Research Center for Development of Far-Infrared Region

Efficient spintronic terahertz emitters:

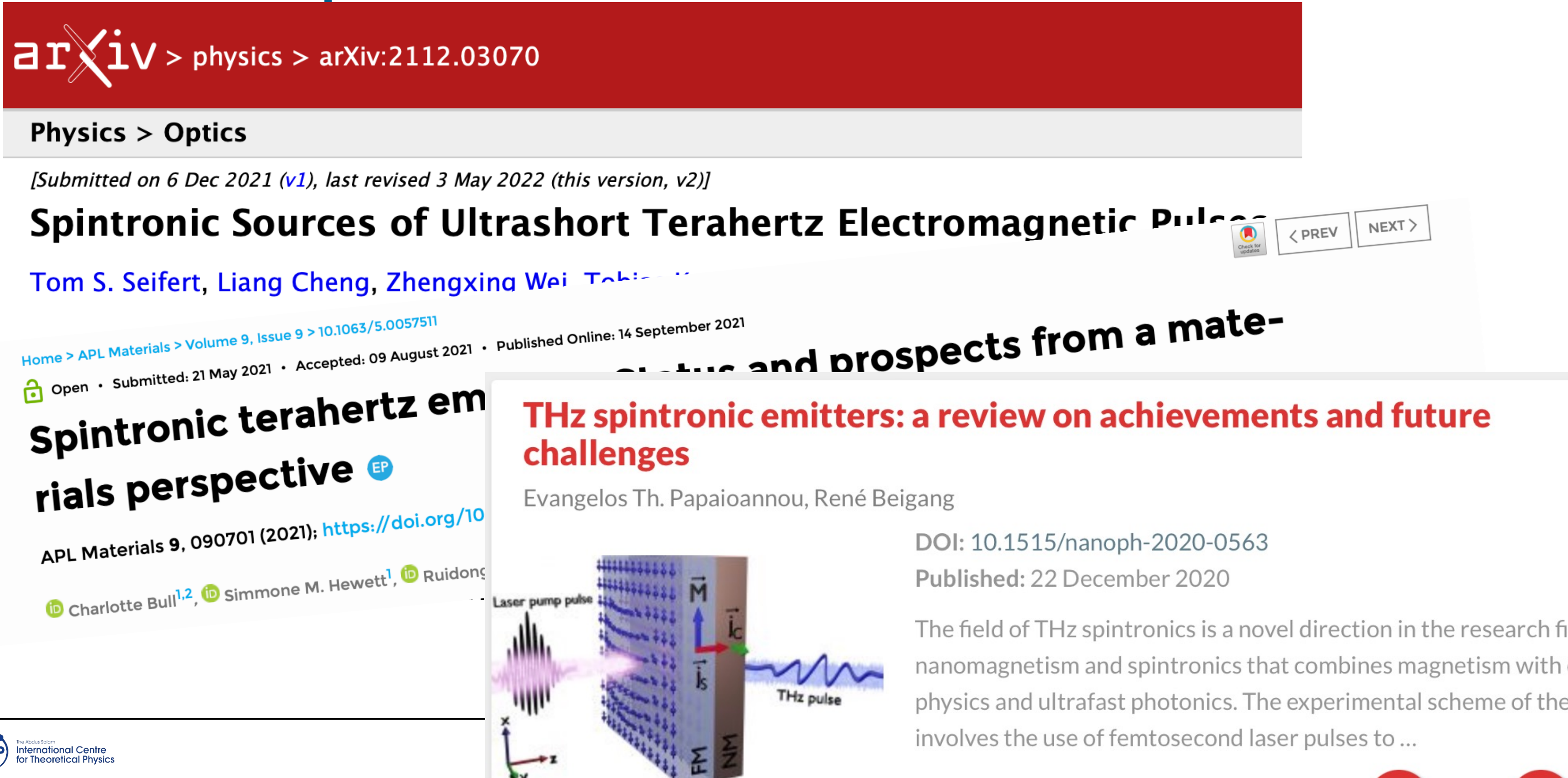

arXiv > physics > arXiv:2112.03070

Physics > Optics

[Submitted on 6 Dec 2021 (v1), last revised 3 May 2022 (this version, v2)]

Spintronic Sources of Ultrashort Terahertz Electromagnetic Pulses

Tom S. Seifert, Liang Cheng, Zhengxing Wei, Tobias K

< PREV NEXT >

Home > APL Materials > Volume 9, Issue 9 > 10.1063/5.0057511

Open • Submitted: 21 May 2021 • Accepted: 09 August 2021 • Published Online: 14 September 2021

Spintronic terahertz emitters: Status and prospects from a materials perspective

APL Materials 9, 090701 (2021); https://doi.org/10

Charlotte Bull[1,2], Simmone M. Hewett[1], Ruidong

THz spintronic emitters: a review on achievements and future challenges

Evangelos Th. Papaioannou, René Beigang

DOI: 10.1515/nanoph-2020-0563

Published: 22 December 2020

The field of THz spintronics is a novel direction in the research fi nanomagnetism and spintronics that combines magnetism with physics and ultrafast photonics. The experimental scheme of the involves the use of femtosecond laser pulses to ...

Efficient spintronic terahertz emitters:

Basic principles and technical realization

Content

Introduction

Femtosecond laser driven THz sources

Spintronics and THz emission

Technical realization

Optimization and typical Results

Outlook and Summary

Efficient spintronic terahertz emitters:
Basic principles and technical realization

Content

Introduction

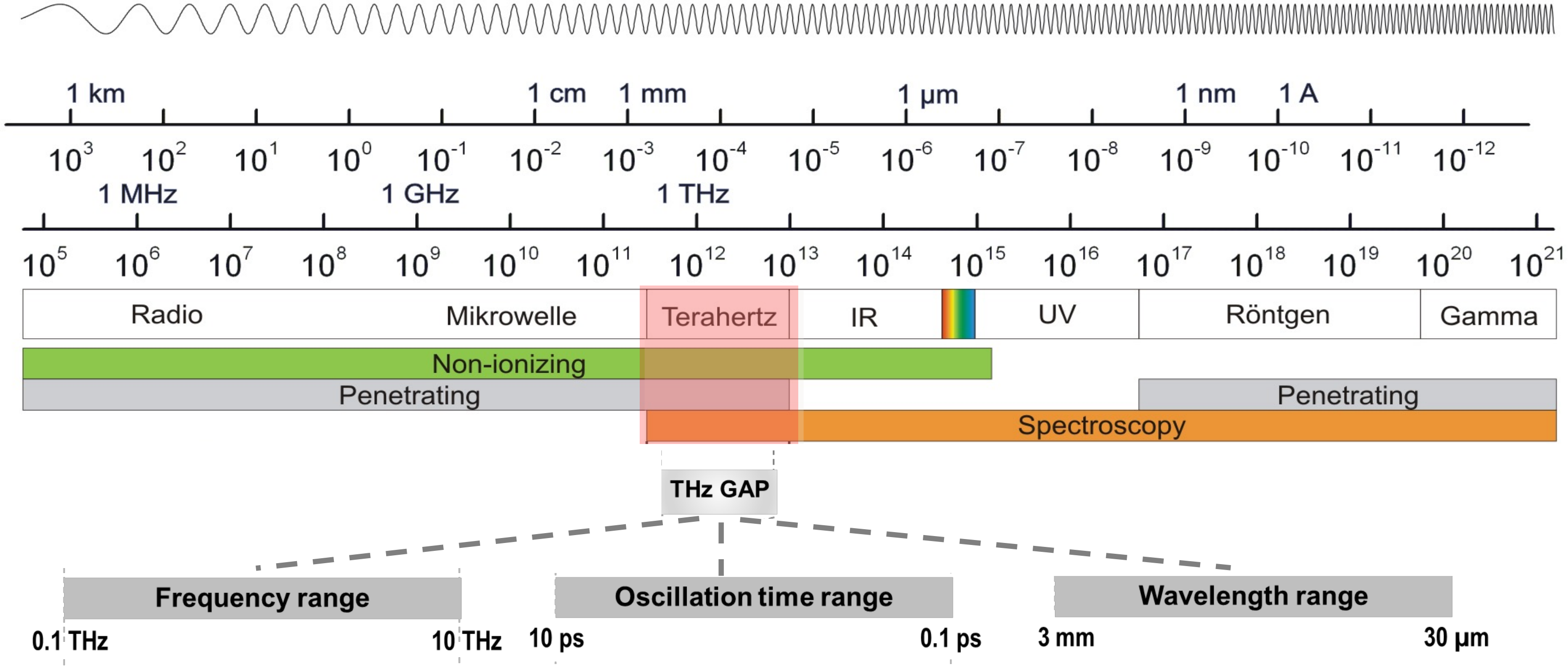

Sources: Fraunhofer IPM (5) Pixelio.de (2), Panasonic (3), Linksys (1), Samsung (1), Smiths Detection (1), QinetiQ (1), Forschungszentrum Rossendorf (1), Richard Bartz (1)

Introduction

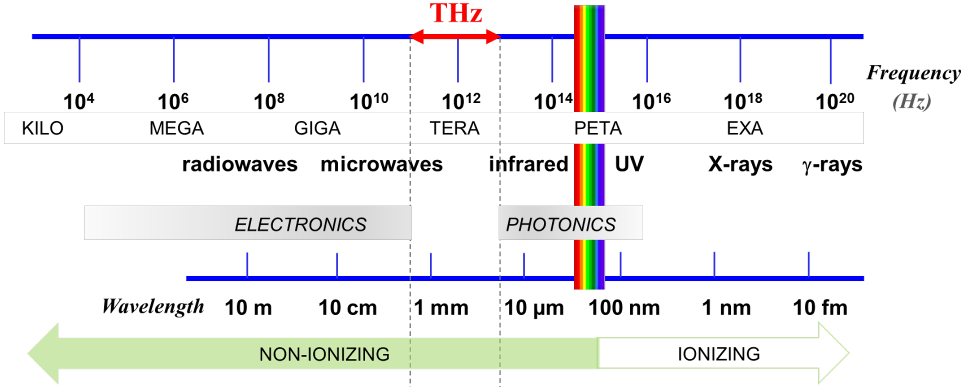

- biomolecular vibrations,
- vibrational motions of organic compounds,
- lattice vibrations in solids,
- intra-band transitions in semiconductors,
- energy gaps in superconductors, …

THz science and technology

- Generation
- Detection
- Components
- THz spectroscopic systems
- THz imaging
- Industrial applications

↓

Efficient THz systems

Typical THz Sources

pulsed

continuous wave

short pulses (< 1 ps)
broad band
spintronic THz emitter
PCS, surface emitter, opt. rectification,…

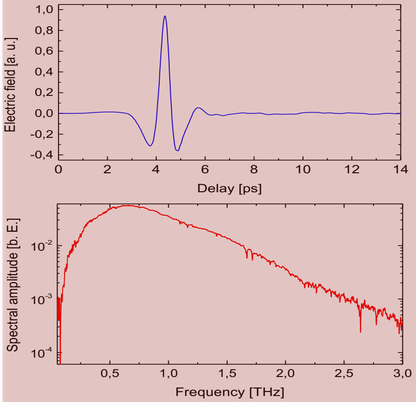

long pulses (>10 ps)
narrow band

opt. rectification in PPLN, GaAs, OPOs, …

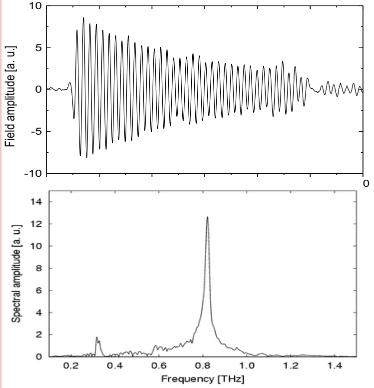

DFG, photomixing,…

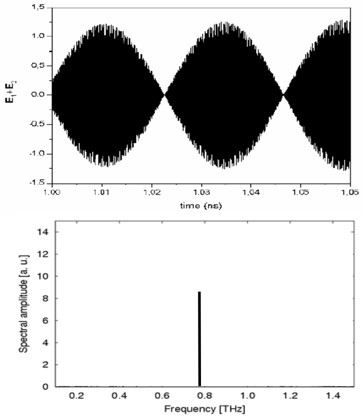

direct lasers:
gas, Ge, QCL, ….
backward oszillators

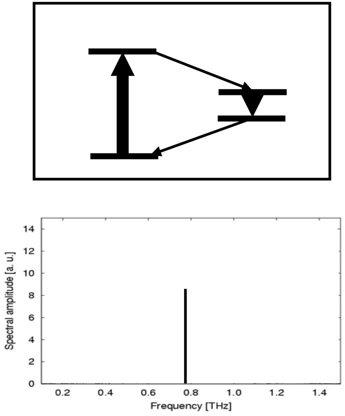

Femtosecond laser-driven THz sources

Photoconductive antenna (PCA)

mechanism: photo-excited carrier acceleratio

Electro-optic crystals – **LiNbO3** and **ZnTe**

mechanism: optical rectification due to second-order nonlinear effect

Semiconductor surface emitters – **GaAs**, **InAs,** and **InSb**

mechanism: surge current either due to surface-depletion field effect (drift) or photo-Dember effect (diffusion)

Air plasma

mechanisms: ponderomotively induced acceleration of electrons and ions upon photoionization, four-wave mixing, plasma current driven by asymmetric laser field

Femtosecond laser-driven THz sources

E_{THz} is proportional to the time-derivative of an induced local charge current J_c

$$E_{THz} \propto \frac{\partial J_c}{\partial t} = \frac{\partial}{\partial t}\left[\underbrace{J_{ph}(t) + \frac{\partial P(t)}{\partial t}}_{\downarrow} + \underbrace{\nabla \times M(t)}_{\downarrow}\right]$$

electric dipol emission

magnetic dipol emission (very weak)

e.g. ultrafast demagnetization of optically excited magnetic structures

Femtosecond laser-driven THz sources

E_{THz} is proportional to the time-derivative of an i ed local charge current J_c

$$E_{THz} \propto \frac{\partial J_c}{\partial t} = \frac{\partial}{} [$$

Ideal THz Emitter:

efficient,
broadband,
low-cost,
and easy-to-use

magnetic dipol emission (very weak)

e.g. ultrafast demagnetization of optically excited magnetic structures

Spintronic Heterostructures as THz Emitters

Ferromagnetic and non-ferromagnetic thin-film layers stacked together

Ultrathin spintronic multilayers emit THz radiation by inverse spin-Hall effect (ISHE)

- ✓ Broadband THz emission (up to 30 THz)
- ✓ Tunable amplitude and polarization of the THz emission
- ✓ No lithography needed
- ✓ Electrical contacts not required
- ✓ Large THz field amplitude at low pump power
- ✓ High optical damage threshold (above 5 mJ/cm²)

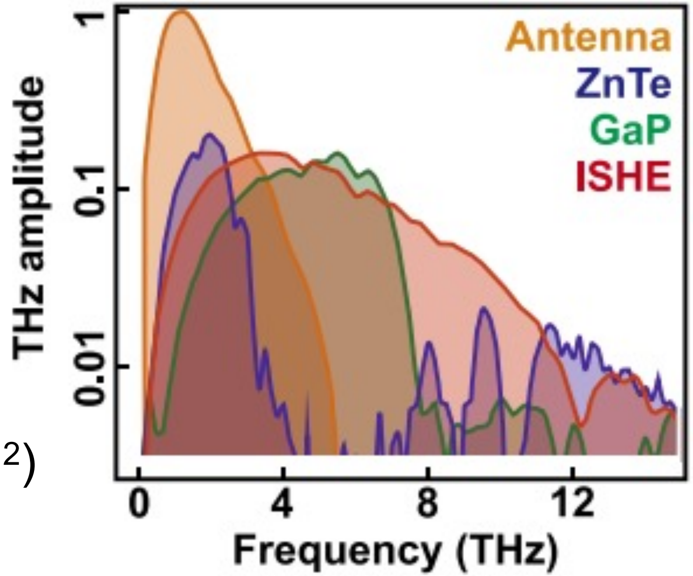

T. Seifert, *et.al.*, Nature Photonics, **10**, 483-488 (2016), G. Torosyan, *et al.*, Scientific Reports, **8**, 1311 1-9 (2018), D. Yang, *et al.*, Advanced Optical Materials, **4**, 1944-1949 (2016).

Efficient spintronic terahertz emitters:
Basic principles and technical realization

Content

Introduction

Femtosecond laser driven THz sources

Spintronics and THz emission

Technical realization

Optimization and typical Results

Outlook and Summary

Photoconductive switch as emitter

$$E(t) \propto \frac{\partial j}{\partial t} \quad j(t) = \frac{\partial P}{\partial t}$$

$$P(t) = N(t) \cdot e \cdot x(t)$$

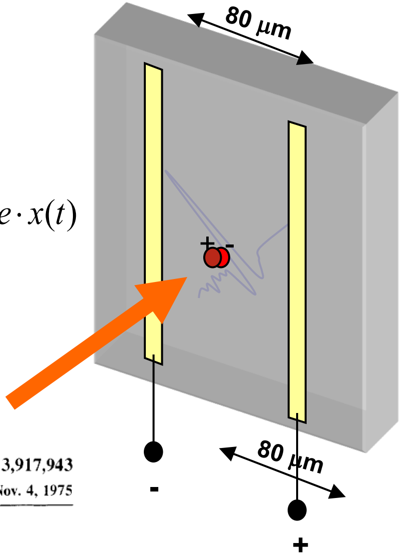

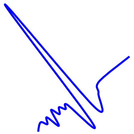

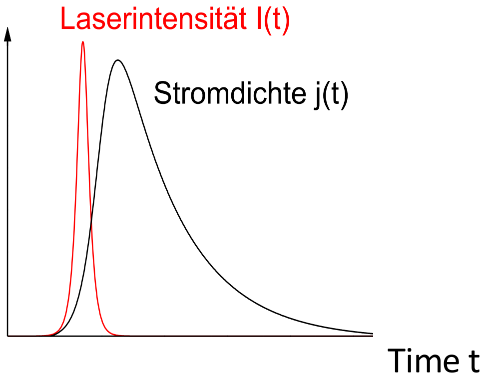

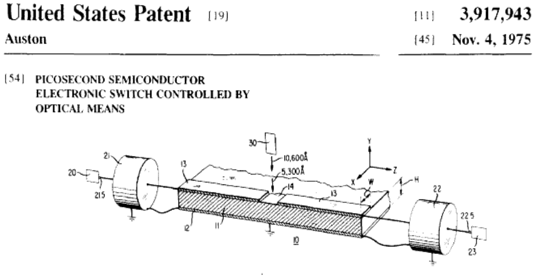

United States Patent [19]
Auston

[11] 3,917,943
[45] Nov. 4, 1975

[54] PICOSECOND SEMICONDUCTOR
ELECTRONIC SWITCH CONTROLLED BY
OPTICAL MEANS

Photoconductive switch as detector

Coherent detection

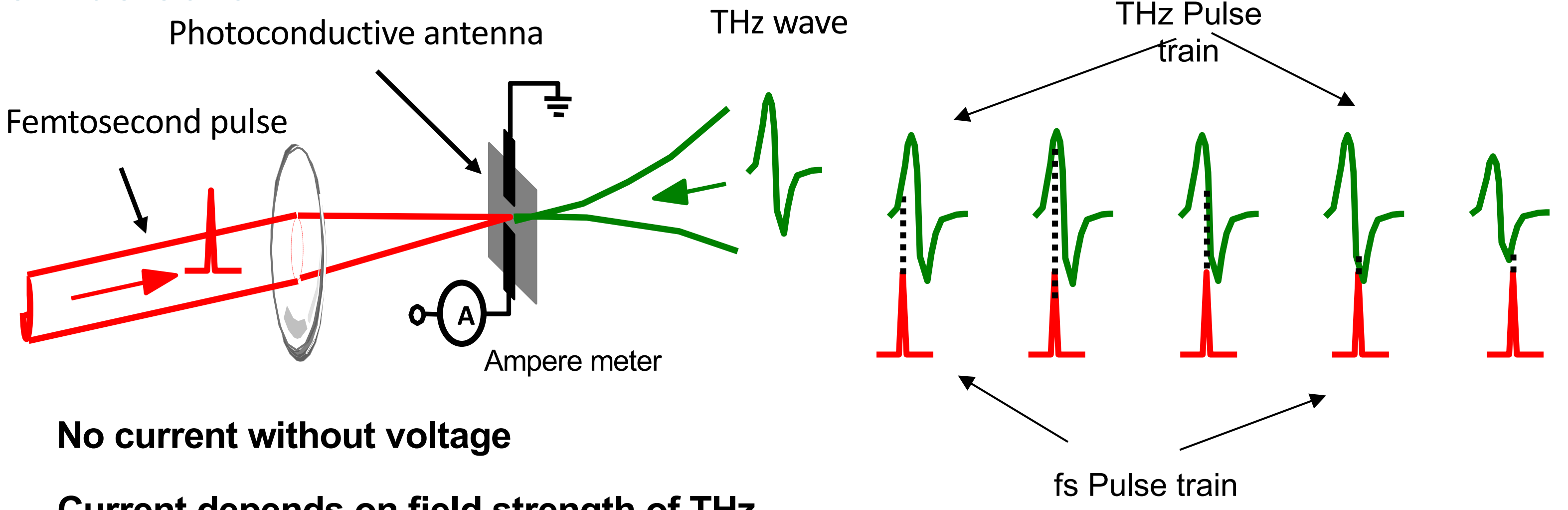

No current without voltage

Current depends on field strength of THz pulse

However:

fs pulse is much shorter than THz pulse (100 x)

Only the instantenous field is accelerating the charges

Temporal sampling of the THz pulse via averaging over many pulses

Photoconductive switch as detector

Coherent detection

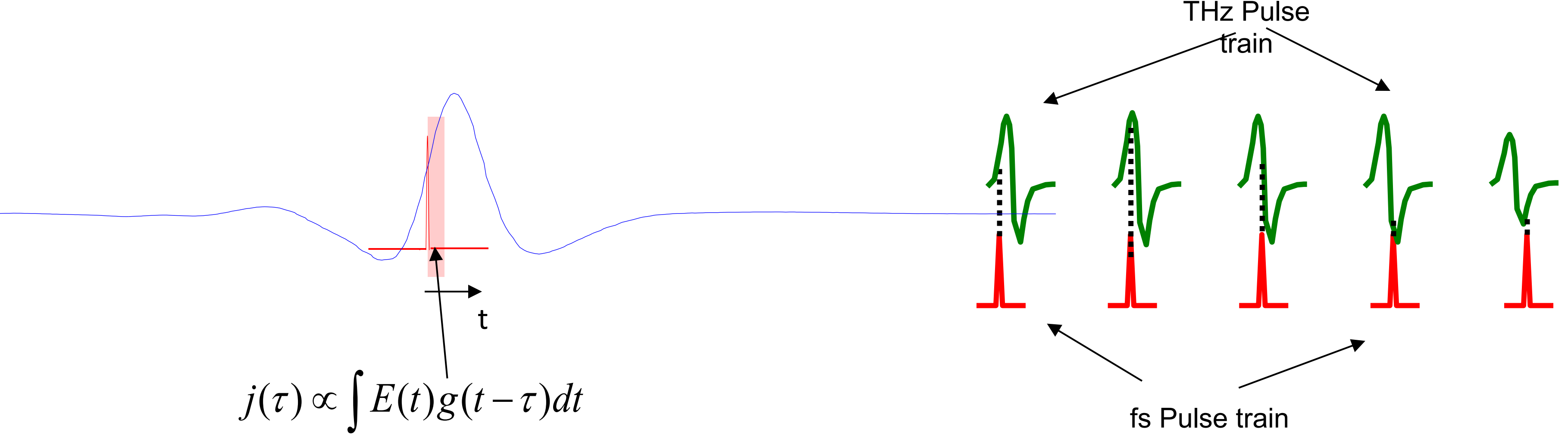

$$j(\tau) \propto \int E(t)g(t-\tau)dt$$

finite length of NIR pulse and carrier lifetime

- ➡ averaging over electric field of THz pulse
- ➡ dipole structure also determines frequency response

Temporal sampling of the THz pulse via averaging over many pulses

Photoconductive Switches as Detector

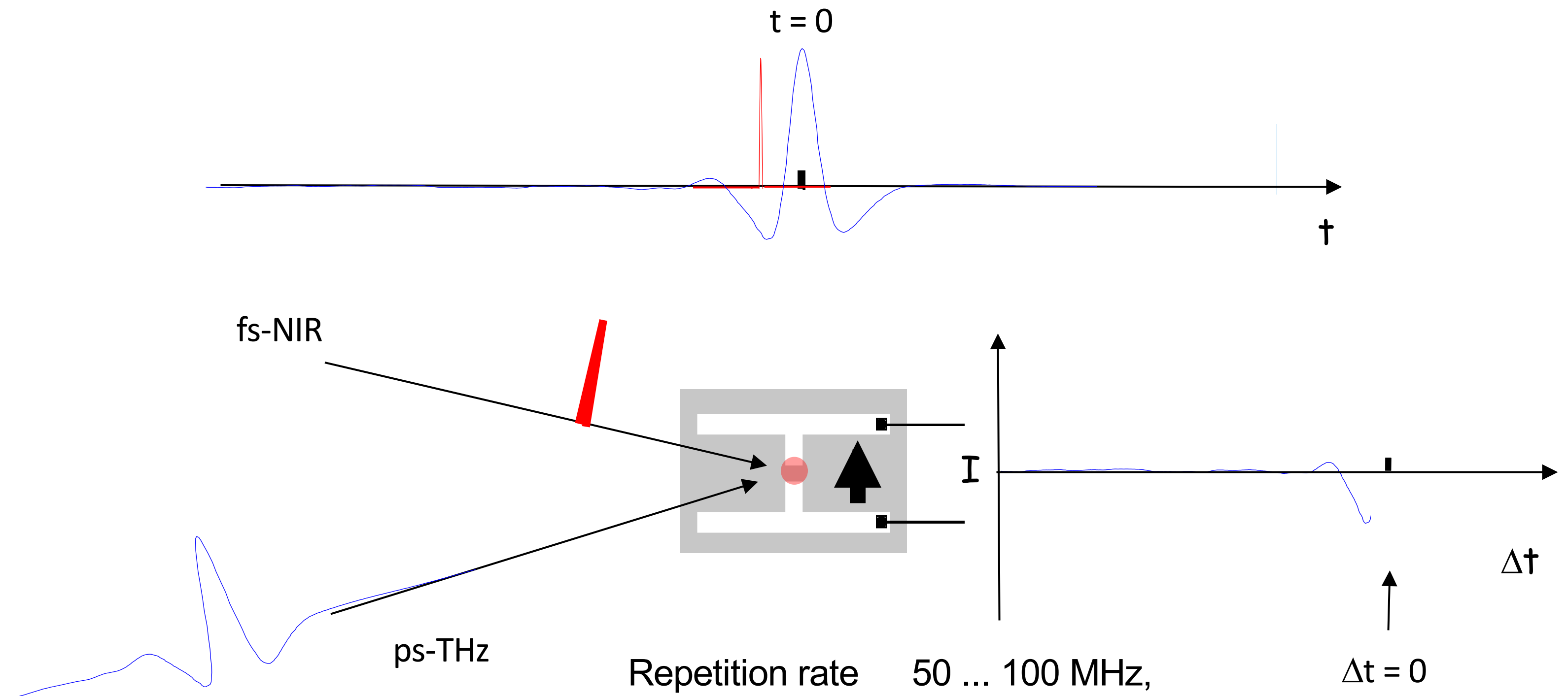

Repetition rate	50 ... 100 MHz,
Sampling rate	1 …10 kHz

Photoconductive Switches as Detector

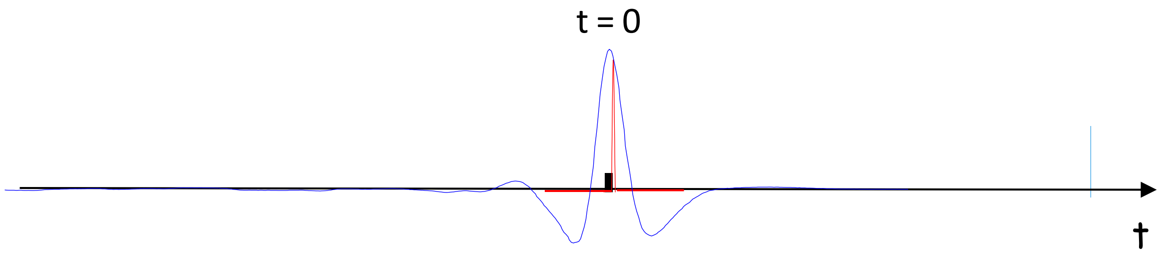

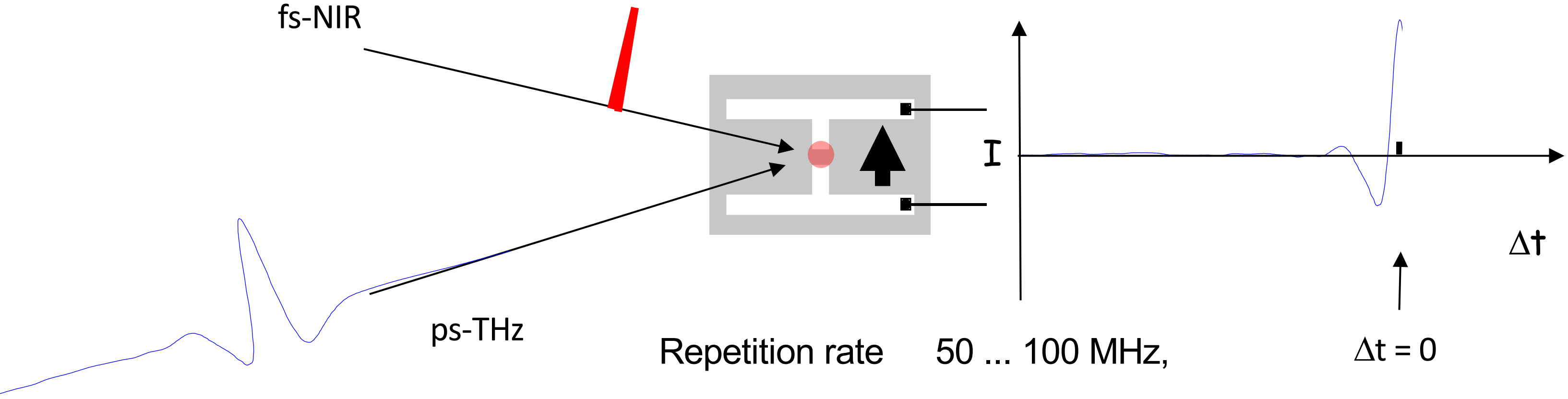

Repetition rate	50 ... 100 MHz,
Sampling rate	1 …10 kHz

THz TDS Principle

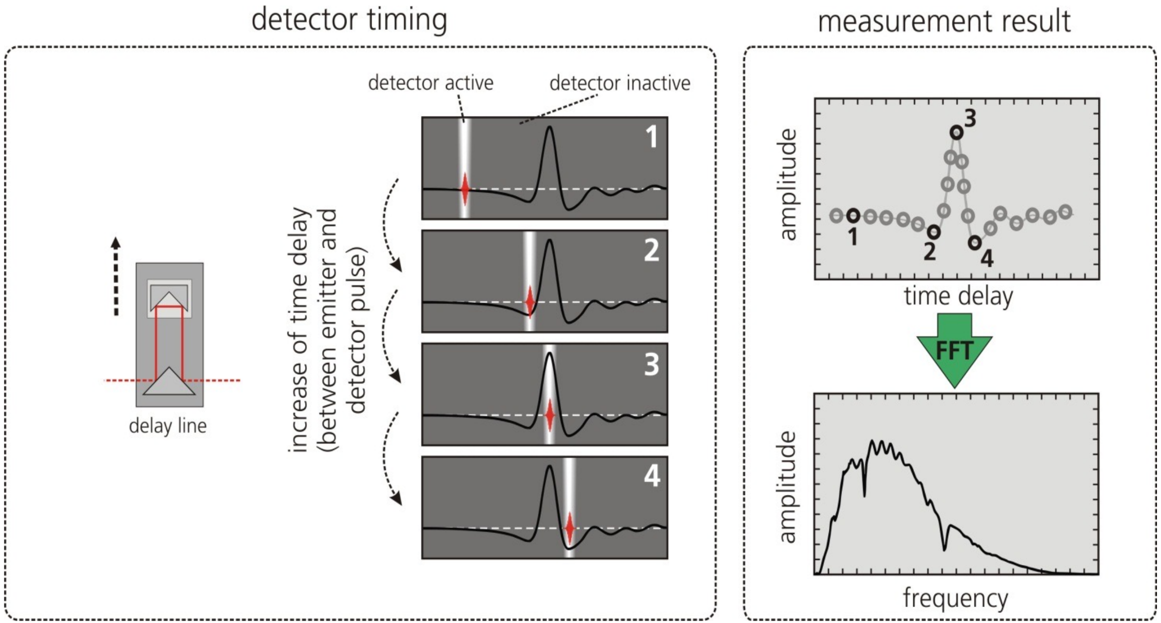

- Detector is active for < 1 ps (activated by fs pulse)
- Sampling by changing the time delay between emitter and detector pulse

Some historical remarks

1986 IBM Press Release:
World's Shortest Electrical Pulses

Internat ss Machines Corporation
Researc
P.O. Box town Heights, New York 10598
D. Arvay
Manager of ical Publicity

CONTACT: Tim Ohsann
(914) 945-3042

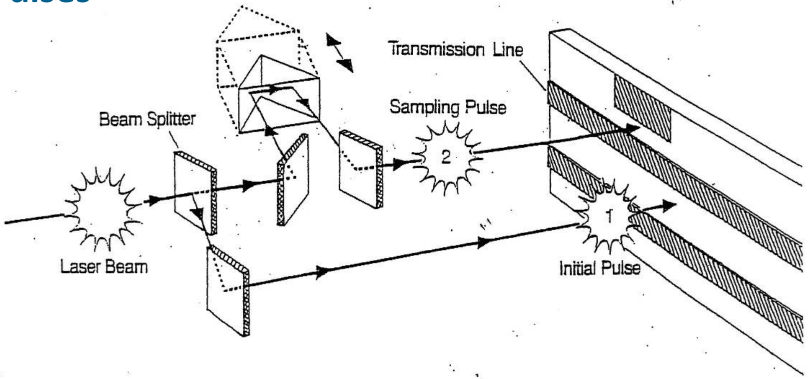

Laser beam pulses are split in two. Researchers can delay one light pulse stream by making it travel a longer distance.

1986

YORKTOWN HEIGHTS, N.Y., June 24 . . . IBM scientists here have made and measured the world's shortest electrical pulses, an important step in designing the ultrafast electronic computer components of the future.

Using a laser and a very fast switch, the scientists produced electrical pulses lasting only one half of a picosecond. A picosecond is one trillionth of a second. Until this experiment, researchers had never broken the "picosecond barrier" with an electronic device.

1986 IBM Press Release:
World's Shortest Electrical Pulses

Interna ss Machines Corporation
Researc
P.O. Box town Heights, New York 10598
D. Arvay
Manager of ical Publicity

CONTACT:

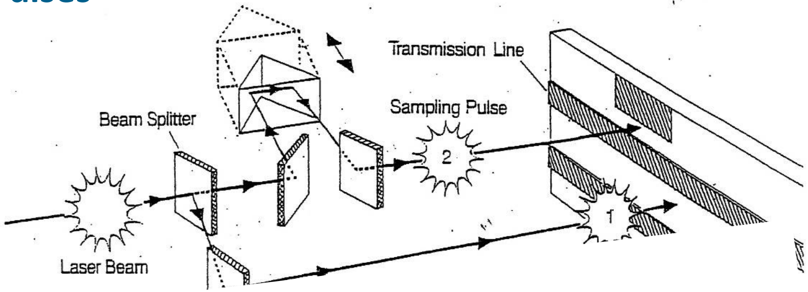

pulse

Where is the THz pulse??

ture.

ast switch, the scientists produced electrical pulses lasting only one half of a picosecond. A picosecond is one trillionth of a second. Until this experiment, researchers had never broken the "pico-second barrier" with an electronic device.

THz pulse from transmission line

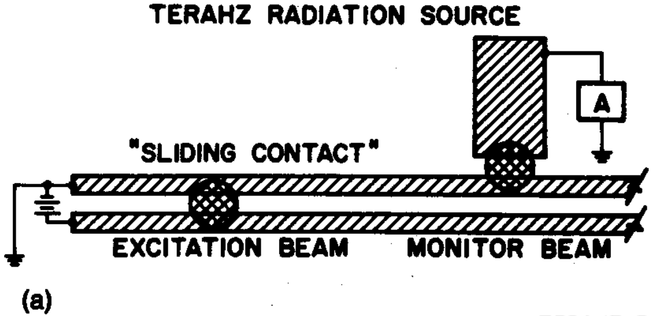

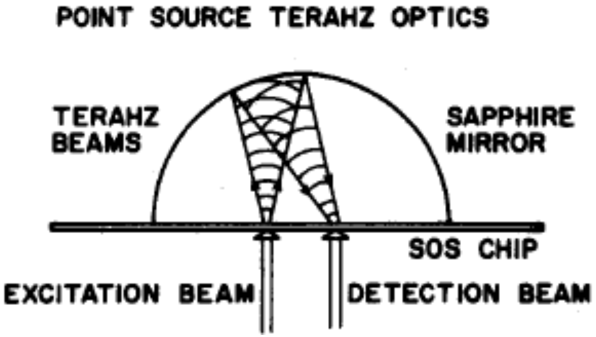

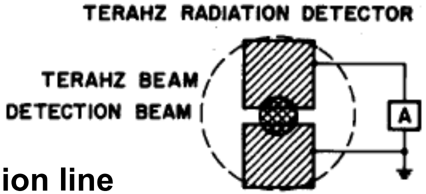

Electrical pulse on transmission line

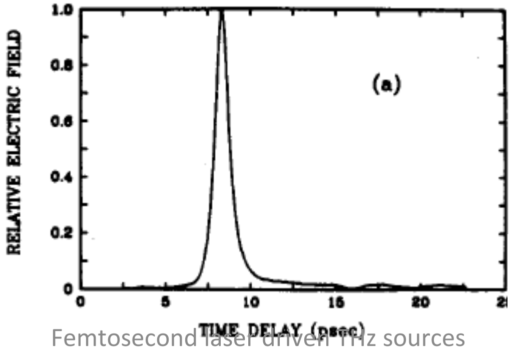

100 ps later …

Radiated pulse

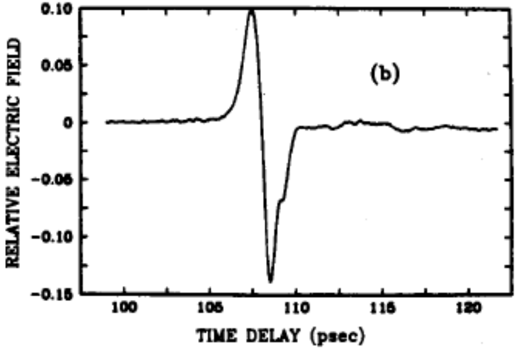

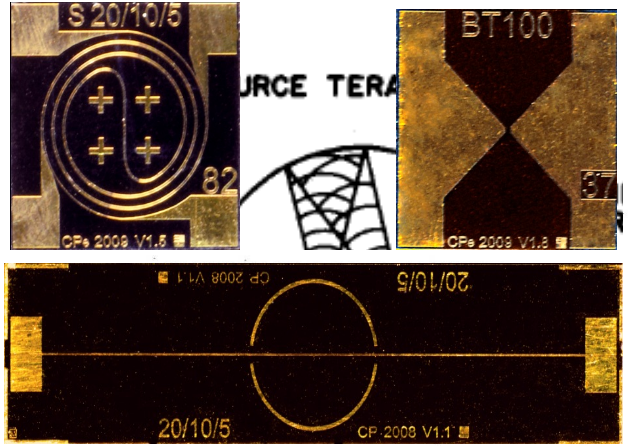

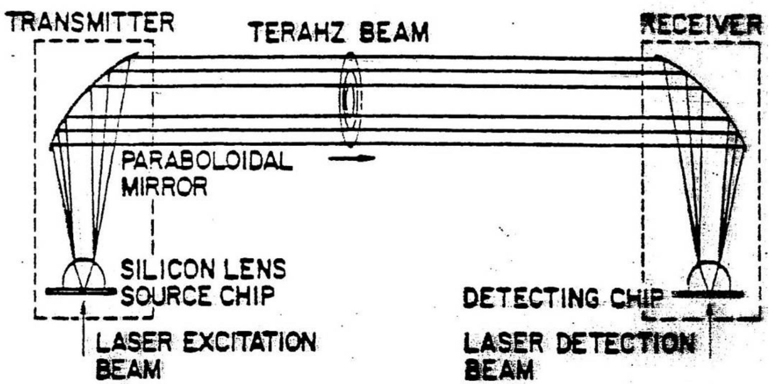

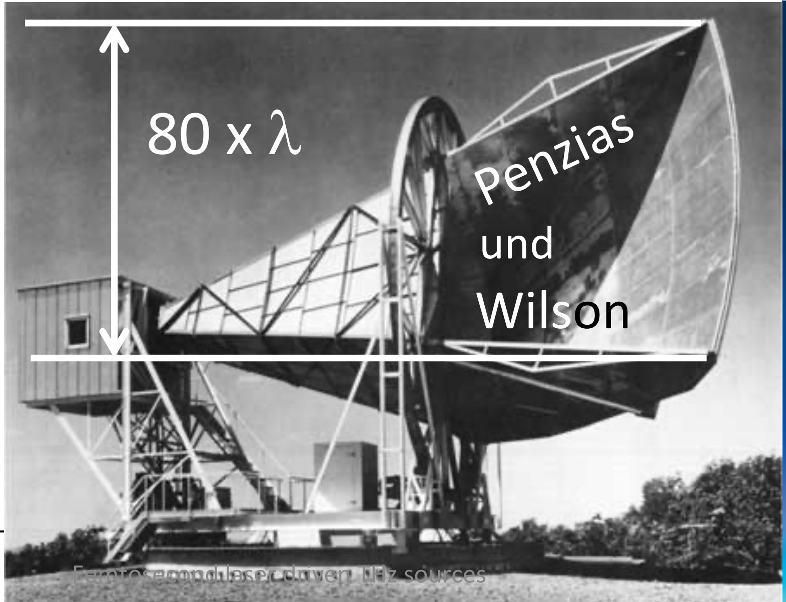
80 x λ

Penzias und Wilson

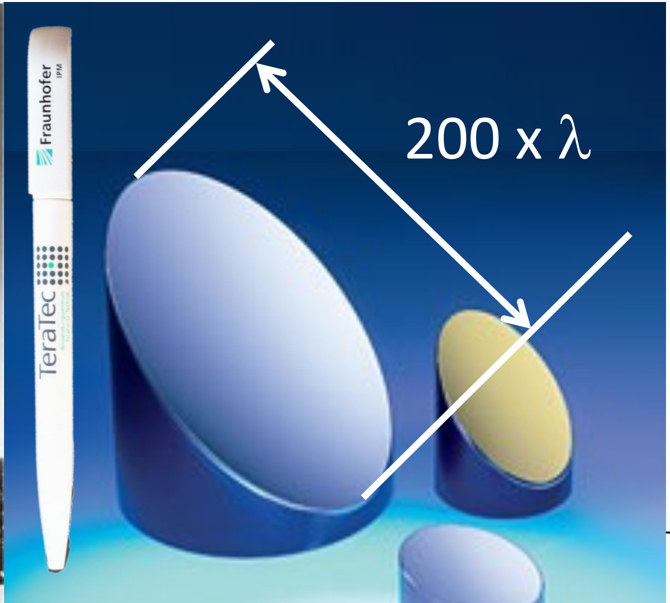

200 x λ

Measuring principle

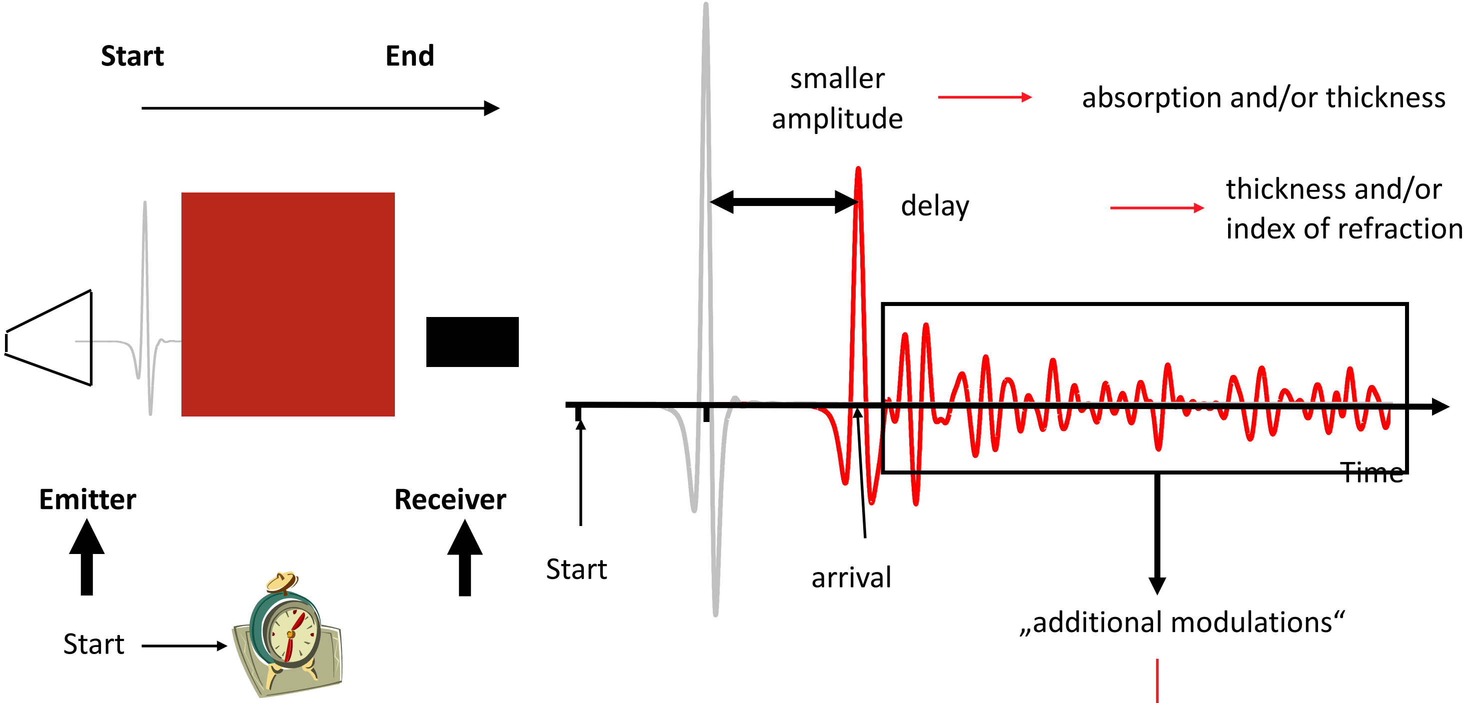

Start

End

Emitter

Receiver

Start

Start

arrival

Time

smaller amplitude → absorption and/or thickness

delay → thickness and/or index of refraction

„additional modulations“

↓

spectroscopic information

Analysis of Terahertz TDS signale

Time domain

Messung des elektrischen Feldes

Pulse length < 1 ps

Signal-to-noise > 10^3:1 (60 dB)

(30 ms integration time)

20 wave forms per second

Fourier Transform

Frequency domain

Spectral amplitude

Phase information

Useful bandwidth

100 GHz < n < 4 THz (30 THz ?)

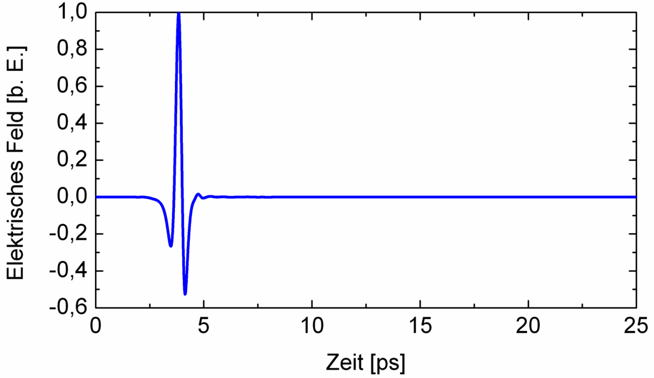

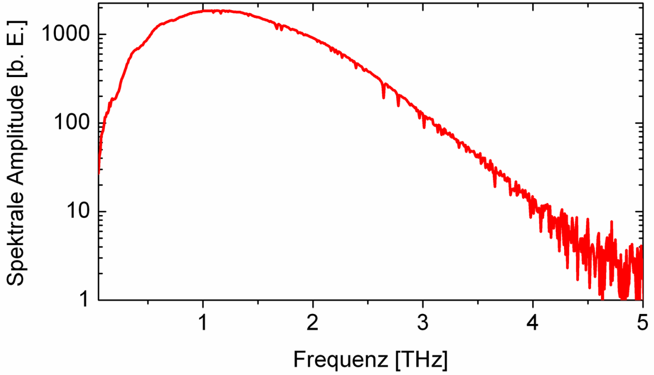

Electromagnetic Waves in Matter

The interaction of electromagnetic radiation with matter: permittivity ε

$$\tilde{\varepsilon}_r(\omega) = \tilde{n}^2(\omega) = \left(n(\omega) + i\kappa(\omega)\right)^2$$

ε_r: Relative permittivity

n: refractive index

κ: extinction coefficient κ

Plane wave in vacuum: $\tilde{E} = E_0 e^{i(kx-\omega t)}$ $(k = \omega / c)$

Plane wave in matter: $\tilde{E} = E_0 e^{i(\tilde{n}(\omega)kx-\omega t)} = E_0 \overbrace{e^{in(\omega)kx}}^{\text{dispersion}} \overbrace{e^{-\kappa(\omega)kx}}^{\text{absorption}} e^{-i\omega t}$

TDS measures: $\tilde{t} = \dfrac{\tilde{E}_{sample}}{\tilde{E}_{ref}} = \dfrac{E_0 e^{i(\tilde{n}kx-\omega t)}}{E_0 e^{i(kx-\omega t)}} = e^{i(\tilde{n}-1)kx}$

Electromagnetic Waves in Matter

TDS measures

$$\tilde{t} = \frac{\tilde{E}_{sample}}{\tilde{E}_{ref}} = \frac{E_0 e^{i(\tilde{n}kx-\omega t)}}{E_0 e^{i(kx-\omega t)}} = e^{i(\tilde{n}-1)kx}$$

Conventional spectroscopy measures:

$$T = \frac{P_{sample}}{P_{ref}} = \frac{\tilde{E}_{sample}\tilde{E}_{sample}^{*}}{\tilde{E}_{ref}\tilde{E}_{ref}^{*}}$$

$$= e^{i(\tilde{n}-1)kx} e^{-i\left(\tilde{n}^{*}-1\right)kx} = e^{-2\kappa kx} = e^{-\alpha x}$$

Absorption is seen, but phase information is lost:
No information on real part of refractive index, n.

Time Domain Spectroscopy of CO

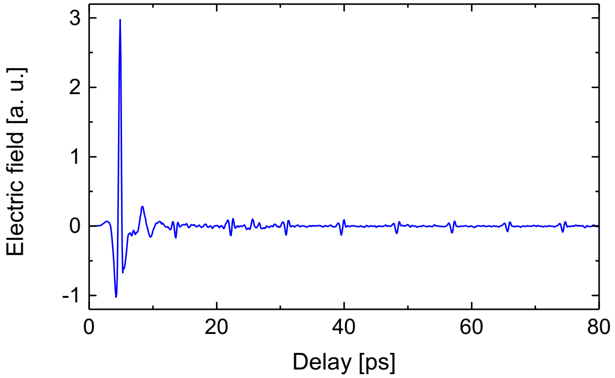

FFT

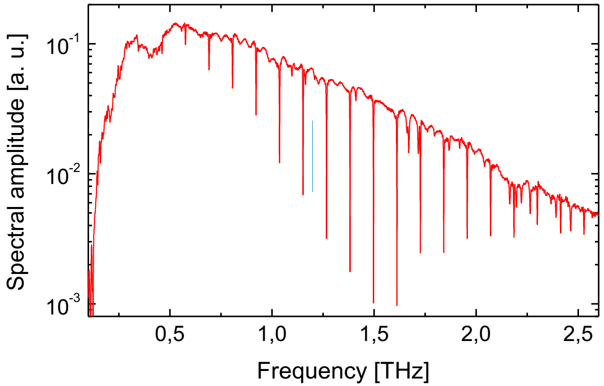

CO spectrum devided by reference spectrum:

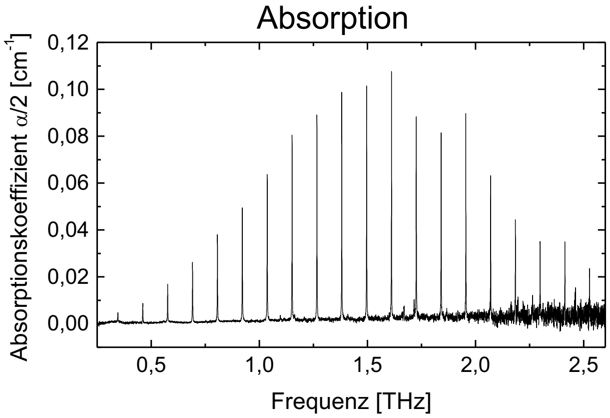

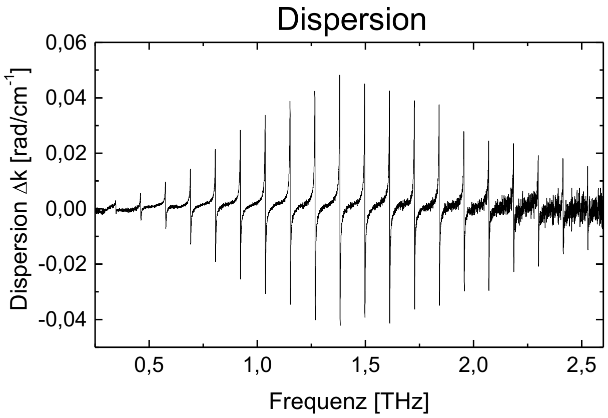

Components of a THz TDS system

Laser	fs Laser, NIR Laser
Emitter	PCS, semiconductors, nonlinear xtals, air plasma
Detector	PCS, EOS
THz Optics	application dependend

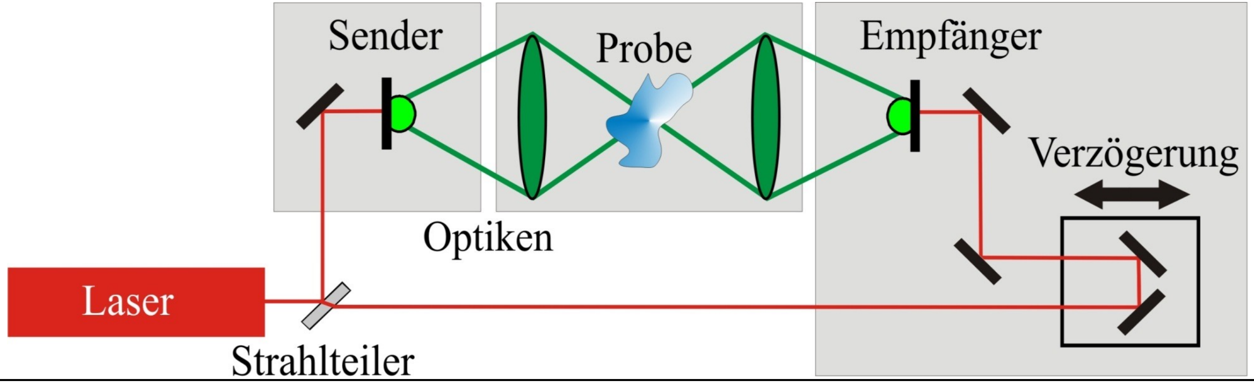

Photoconductive switch

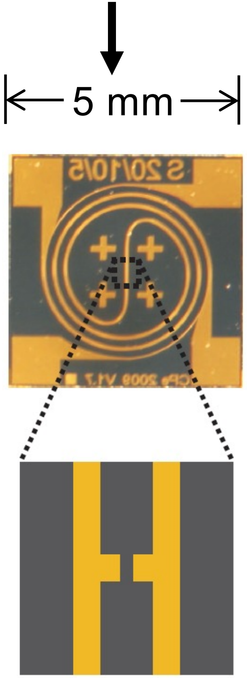

Application of Broadband THz Radiation

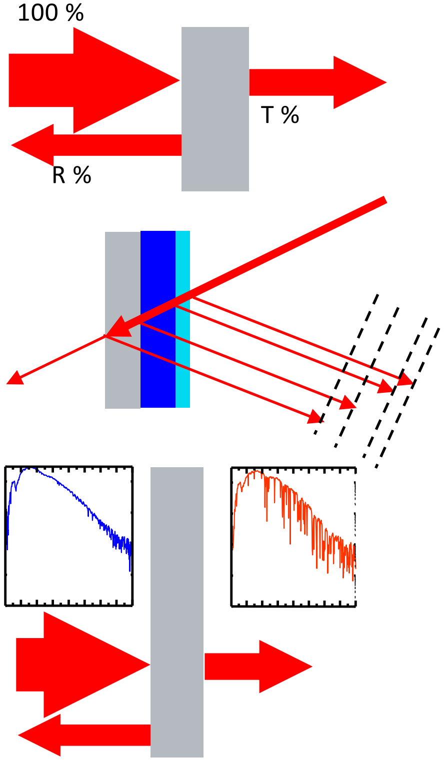

Intensity

(Amplitude and phase)

transmission & reflection

surface, absorption,

foreign bodies, voids, ….

Time structure

tomography

layer thickness,

boundaries, ...

Amplitude & Phase

spectroscopy

identification,

content,

concentration, ...

Application of Broadband THz Radiation

Intensity
(Amplitude and phase)

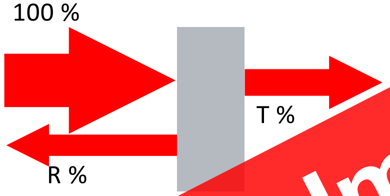

transmission & reflection
surface absorption,
foreign bodies, voids, ….

Hyperspectral Imaging

Time structure

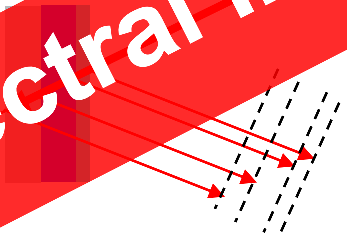

tomography
layer thickness,
boundaries, ...

Amplitude & Phase

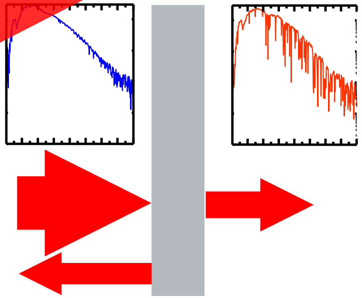

spectroscopy
identification,
content,
concentration, ...

Hyperspectral Imaging

Mock-up letter bomb

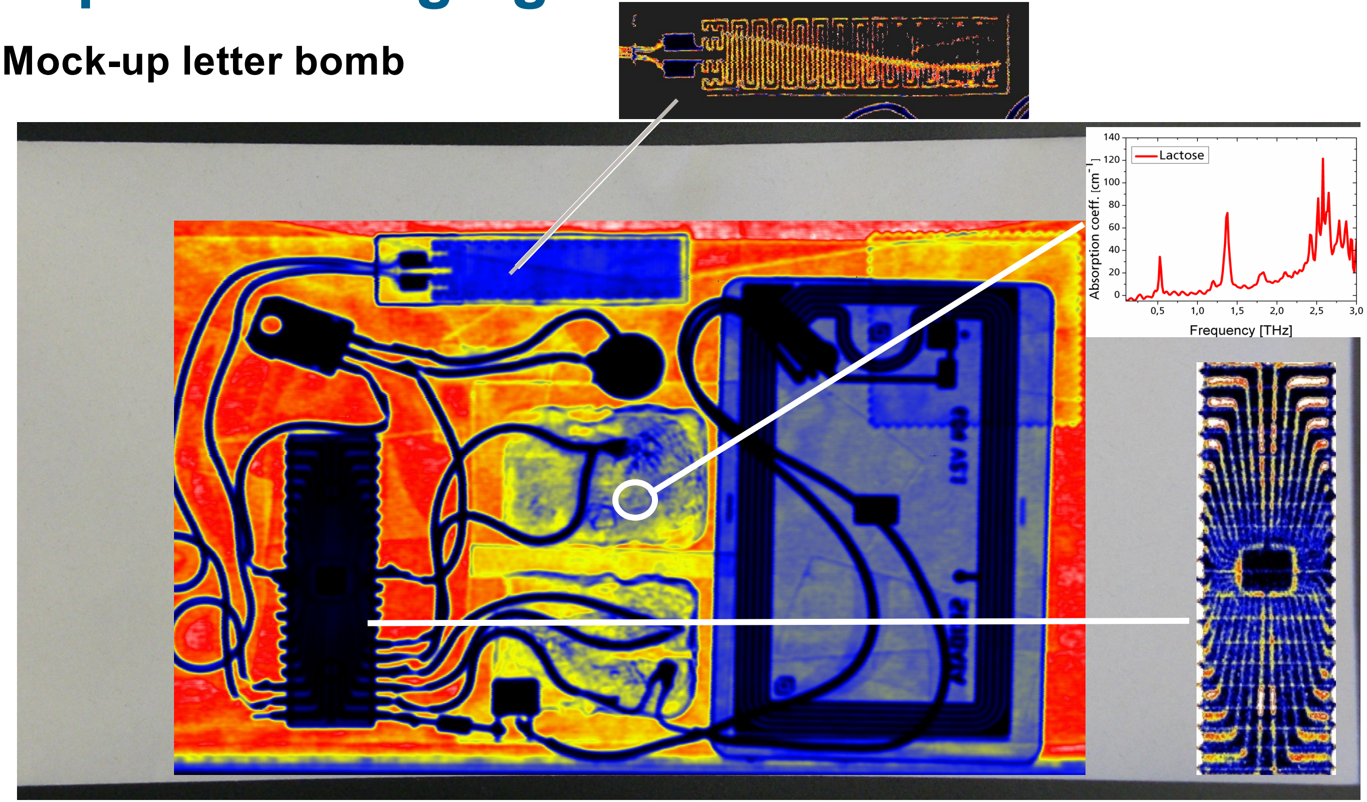

Hyperspectral Imaging

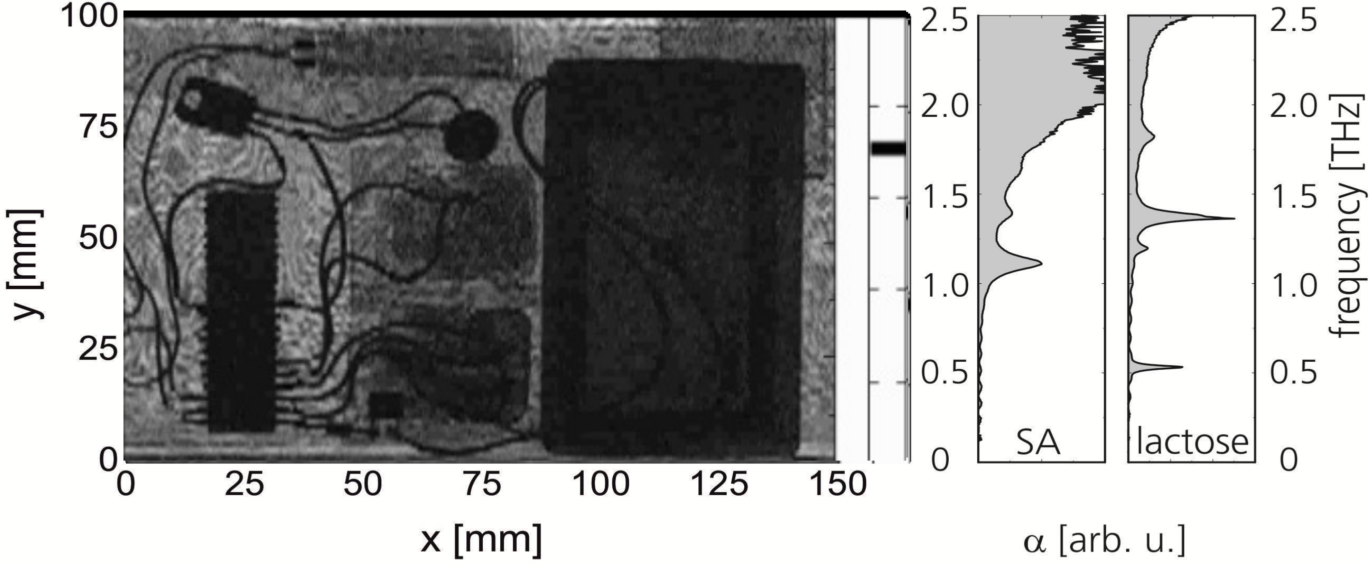

Hyperspectral Imaging

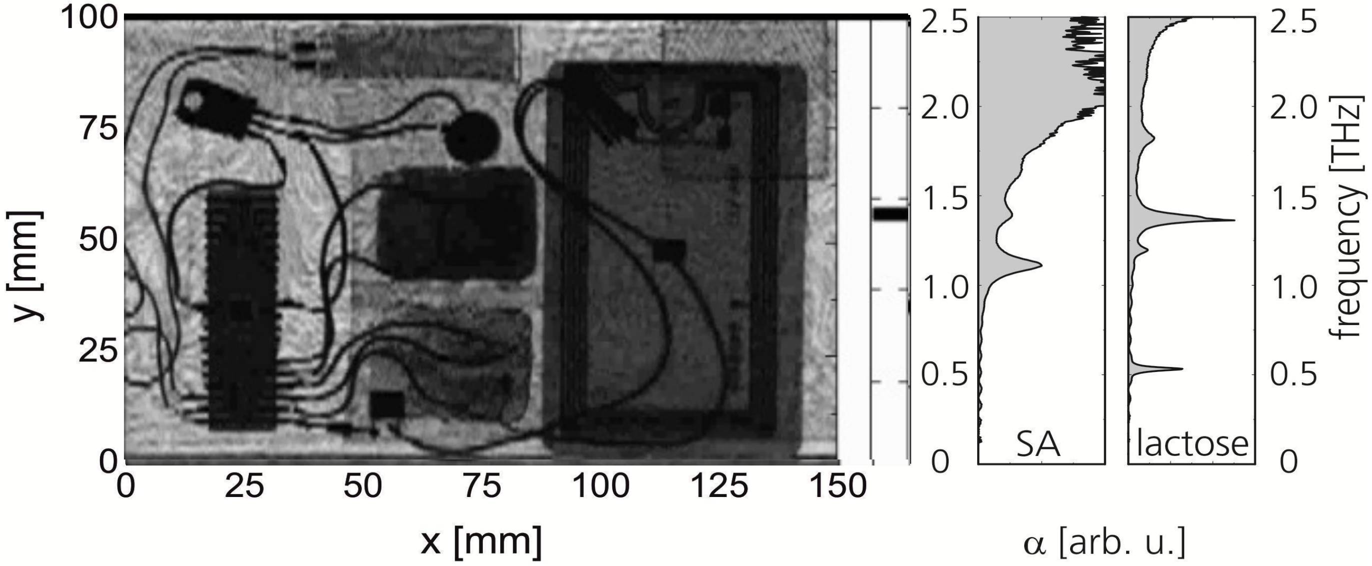

Hyperspectral Imaging

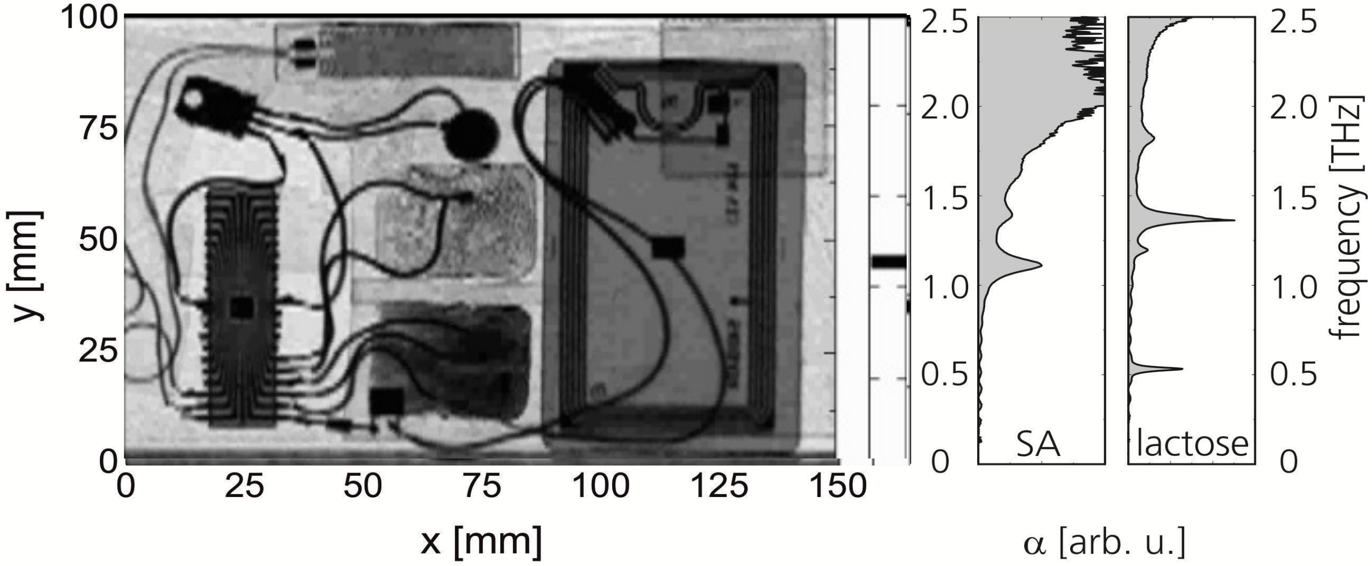

Hyperspectral Imaging

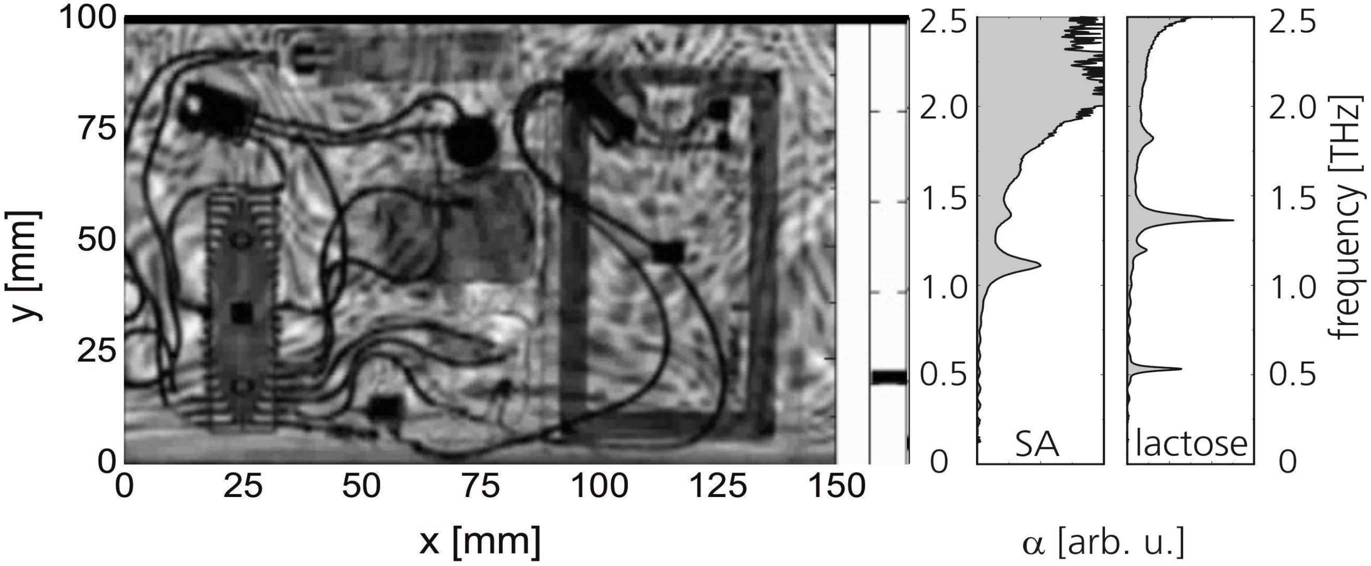

Efficient spintronic terahertz emitters:
Basic principles and technical realization

Content

Principle of THz generation

Inverse Spin Hall Effect ISHE

- Optical pulse generates spin-up and spin-down electrons in magnetic material

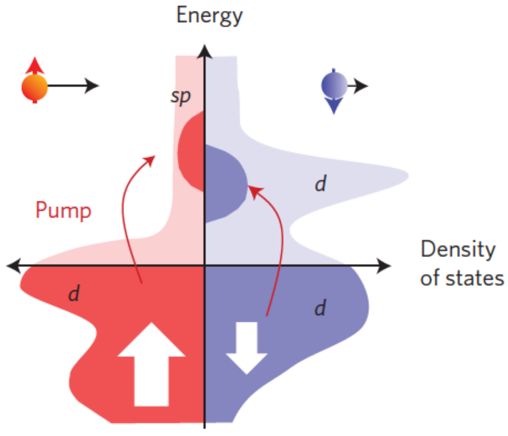

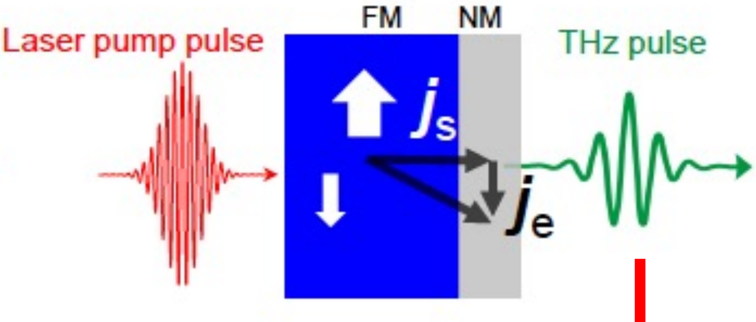

- Spin-orbit coupling separates spin-up and spin-down electrons
- Spin current is converted into electrical current in adjacent non-magnetic material (ISHE)

- Transient current gives rise to THz emission

T. Kampfrath et al., Nature Nanotechnology, 256 (2013), Saitoh et al. Appl. Phys. Lett. 88, 182509 (2006)

Principle of THz generation

Inverse Spin Hall Effect ISHE

- Optical pulse generates spin-u[illegible] spin-down electrons in magnetic material

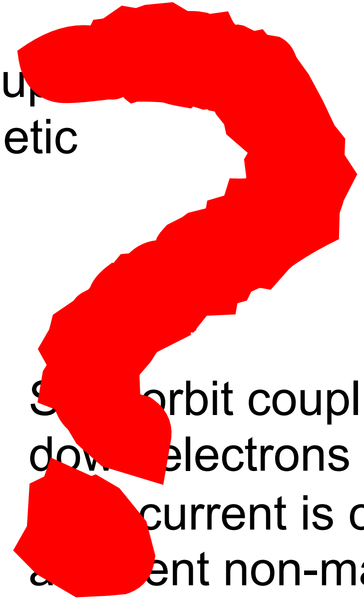

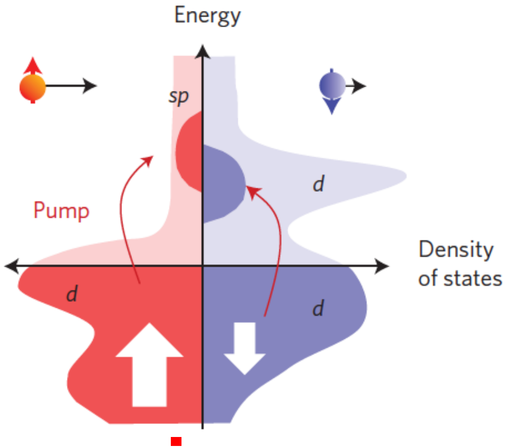

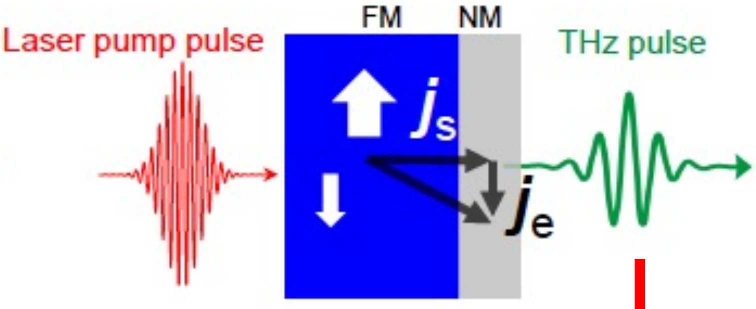

- S[illegible]orbit coupling separates spin-up and spin-dow[illegible]electrons
- [illegible] current is converted into electrical current in a[illegible]ent non-magnetic material (ISHE)

- Transient current gives rise to THz emission

T. Kampfrath et al., Nature Nanotechnology, 256 (2013), Saitoh et al. Appl. Phys. Lett. 88, 182509 (2006)

Electric and Spin currents

„Normal“ metal:

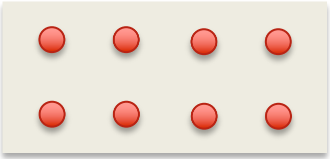

● mobile electrons

metallic conductor in equilibrium

Ohm‘s law: $\vec{j} = \sigma \cdot \vec{E}$

With external electric field $\vec{E}$ …

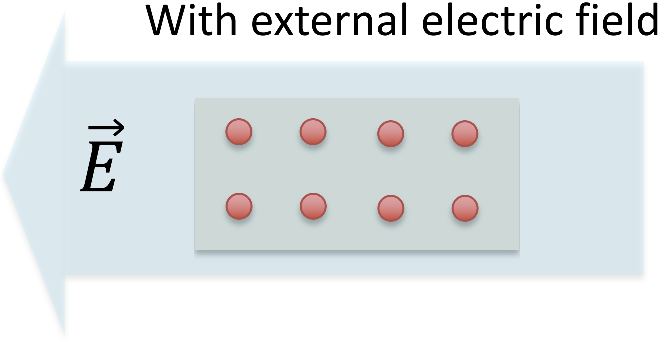

… charge current $\vec{j}_c$

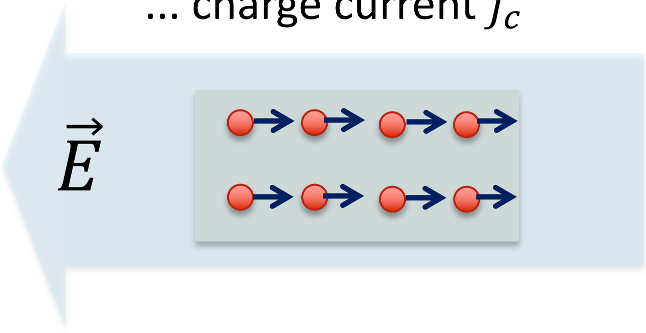

Electric and Spin currents

„Normal“ metal including Spin:

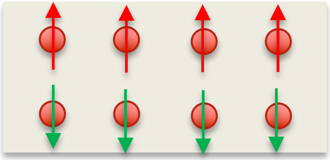

● mobile electrons

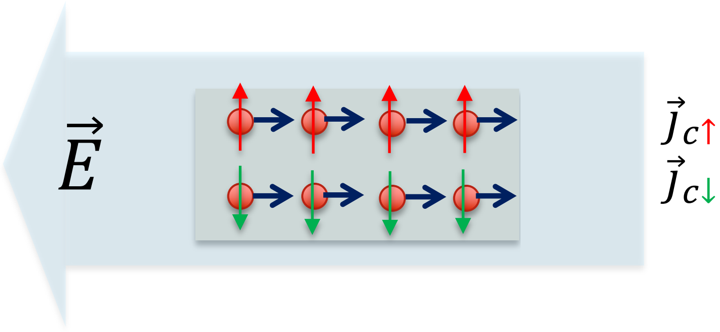

No magnetic order

Mott‘s two spin current model:
Charge currents from electrons with different spin are independent and simply add:

$$\vec{j}_{c\uparrow} = \sigma_{\uparrow} \cdot \vec{E}$$
$$\vec{j}_{c\downarrow} = \sigma_{\downarrow} \cdot \vec{E}$$

$$\vec{j}_{c} = \vec{j}_{c\uparrow} + \vec{j}_{c\downarrow} = (\sigma_{\uparrow} + \sigma_{\downarrow}) = \sigma \cdot \vec{E}$$

Electric and Spin currents

„Normal“ metal including Spin:

Charge **and** spin transport!

Charge transport:

$$\vec{j}_c = \vec{j}_{c\uparrow} + \vec{j}_{c\downarrow} = (\sigma_\uparrow + \sigma_\downarrow) = \sigma \cdot \vec{E}$$

$$\vec{j}_{c\uparrow} = \vec{j}_{c\downarrow} = {}^{\vec{j}_c}/_2$$

Spin transport:

$$\boxed{\vec{j}_s = \frac{+{}^{\hbar}/_2}{e} \cdot \vec{j}_{c\uparrow} + \frac{-{}^{\hbar}/_2}{e} \cdot \vec{j}_{c\downarrow} = 0}$$

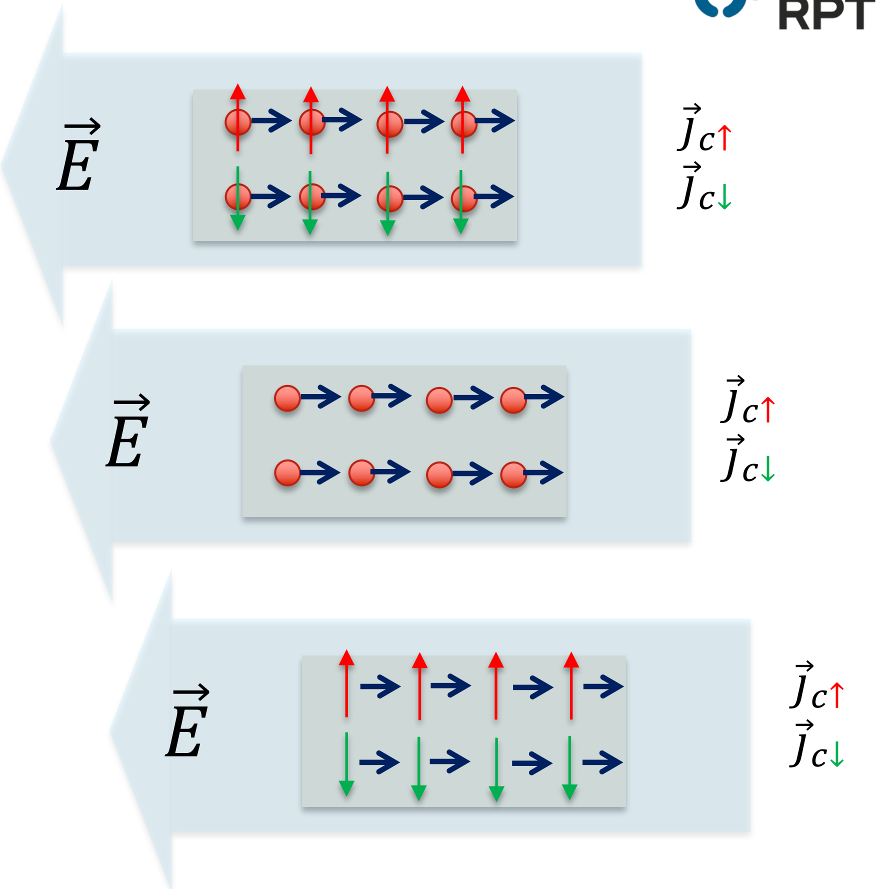

Electric and Spin currents

Ferromagnetic metal including Spin:

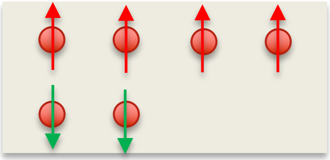

● mobile electrons

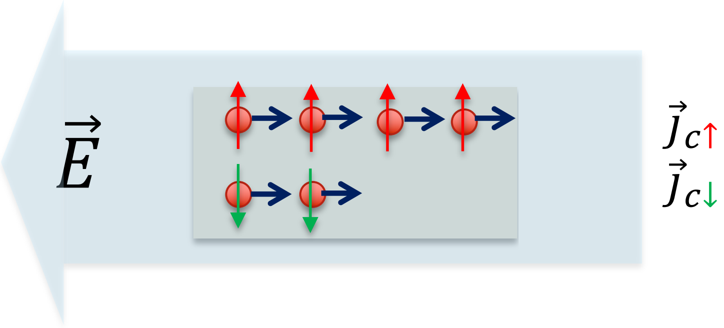

Charge transport:

$$\vec{j}_c = \vec{j}_{c\uparrow} + \vec{j}_{c\downarrow} = (\sigma_\uparrow + \sigma_\downarrow) \cdot \vec{E} = \sigma \cdot \vec{E}$$

but $\vec{j}_{c\uparrow} \neq \vec{j}_{c\downarrow}$

Spin current:

$$\vec{j}_s = \frac{+\hbar/2}{e} \cdot \vec{j}_{c\uparrow} + \frac{-\hbar/2}{e} \cdot \vec{j}_{c\downarrow} \neq 0$$

Non zero charge current **AND** non zero spin current!

Electric and Spin currents

Pure Spin current ?

„Normal" metal including Spin:

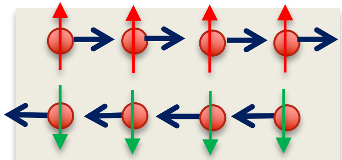

$\vec{j}_{c\uparrow}$

$\vec{j}_{c\downarrow}$

$$\vec{j}_c = \vec{j}_{c\uparrow} + \vec{j}_{c\downarrow} = 0$$

$$\vec{j}_s = \frac{+\hbar/2}{e} \cdot \vec{j}_{c\uparrow} - \frac{-\hbar/2}{e} \cdot \vec{j}_{c\downarrow} = 2\frac{+\hbar/2}{e} \cdot \vec{j}_{c\uparrow} \neq 0$$

Pure Spin current !

.... How can we convince electrons to move in opposite directions depending on their spin orientation? → **Spin dependent scattering**

Spin dependent scattering

„Normal“ scattering

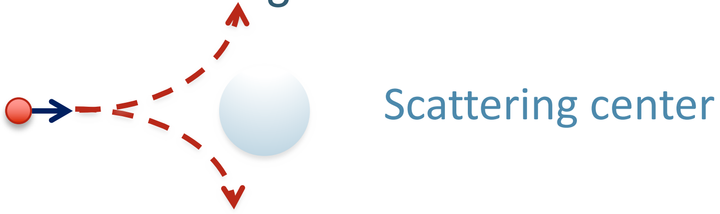

Symmetric scattering in the scattering plane (Rutherford type scattering)

Spin dependent scattering

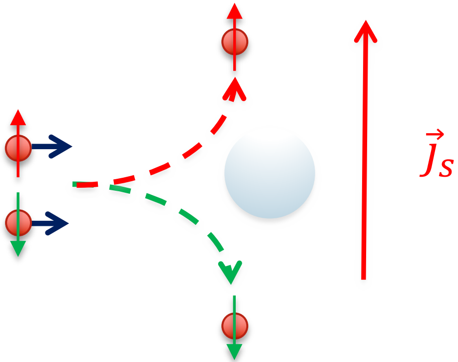

Transverse spin current $\vec{J}_s$

„Spin Hall Effect (SHE)“

However, no charge current if $\vec{J}_{c\uparrow} = \vec{J}_{c\downarrow}$

Spin Hall Effect SHE

Spin dependent scattering

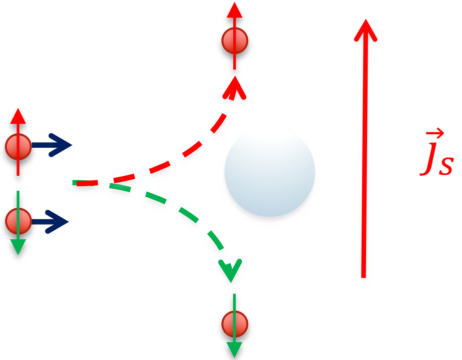

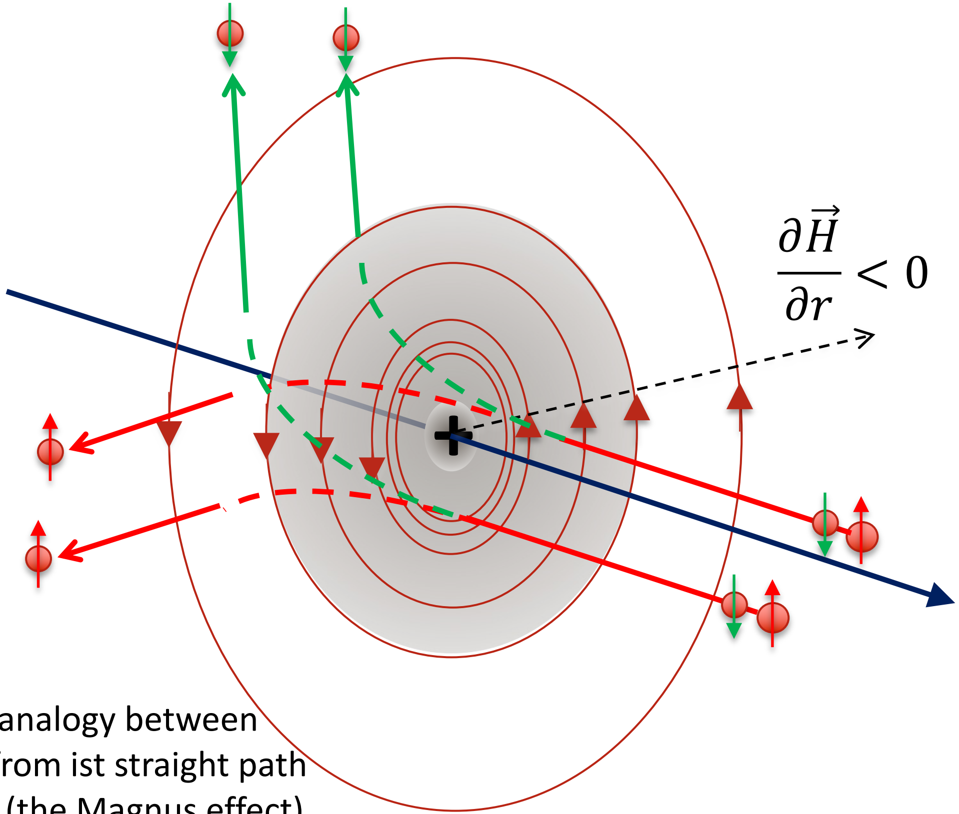

Electrical current $\vec{j}_c$ is
converted into spin current $\vec{j}_s$

One can intuitively understand this effect by using the analogy between an electron and a spinning tennis ball, which deviates from ist straight path in air in a direction depending on the sense of rotation (the Magnus effect).

J. Stöhr and H. C. Siegmann, Springer series in Solid State Sciences 151, Magnetism

Inverse Spin Hall Effect ISHE

Ferromagnetic metal in contact with normal metal

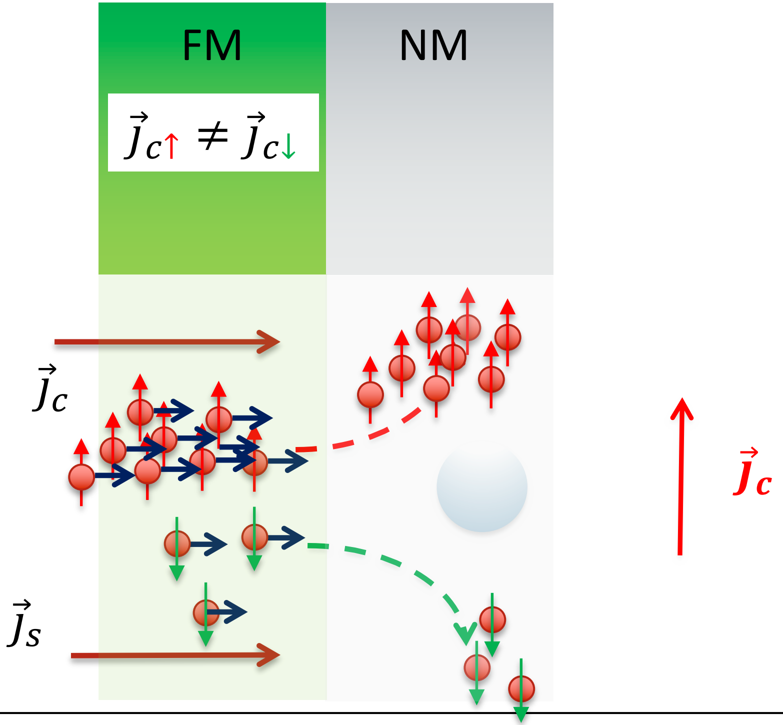

Spin current is partially converted into transient charge current

$$\vec{j}_c = \theta_{SH} \cdot \vec{j}_s \times \frac{\vec{M}}{|\vec{M}|} \qquad \theta_{SH} = \frac{|\vec{j}_c|}{|\vec{j}_s|}$$

Spin-Hall angle θ_{SH}

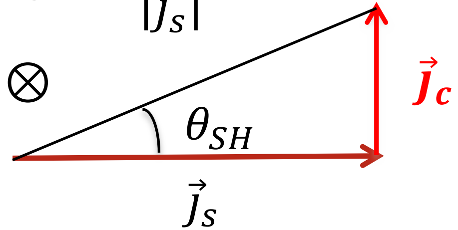

Spin current $\vec{j}_s$ is converted into electric current $\vec{j}_c$ perpendicular to $\vec{j}_s$ and $\vec{M}$

Step 1: Spin current in Fe

Fe: energy bands shifted for ↑e⁻ and ↓e⁻

Highest density in d-band for ↑e⁻ near Fermi level, for ↓e⁻ beneath

Optical pulse generates spin-up and spin-down electrons in magnetic material

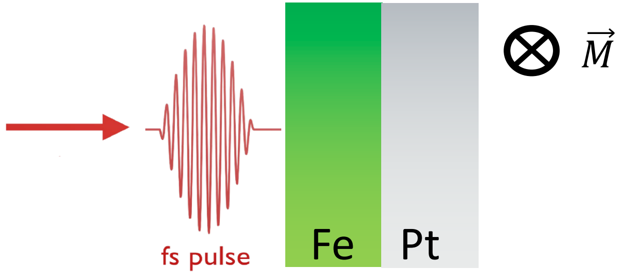

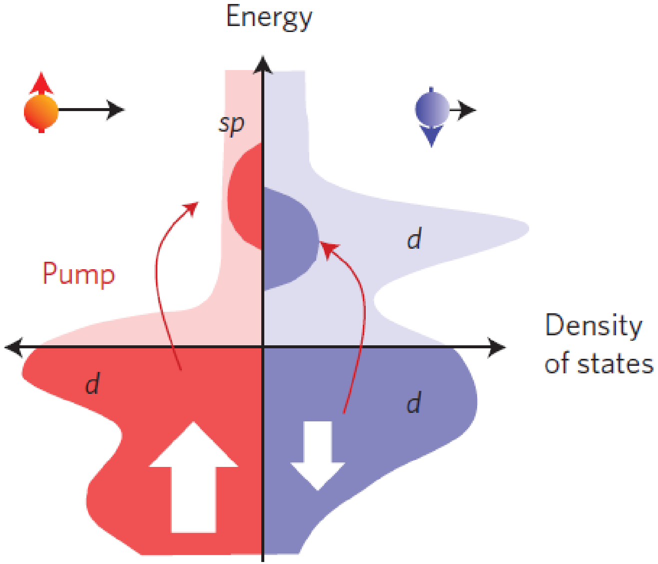

→ ↑e⁻ higher excited than ↓e⁻

→ ↑e⁻ higher E_k on average

→ spin current $\vec{j}_s$

T. Kampfrath *et al.*, Nat. Nanotechnol. **8**, 256 (2013)

Step 2: THz Generation in Fe/Pt Bilayers

e$^-$ diffuse in Pt layer

➡ $\vec{j}_s$ in both layers

ISHE converts $\vec{j}_s$ into charge current $\vec{j}_c$ in Pt:

$$\vec{j}_c = \theta_{SH} \cdot \vec{j}_s \times \frac{\vec{M}}{|\vec{M}|}$$

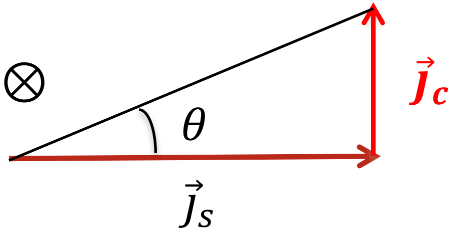

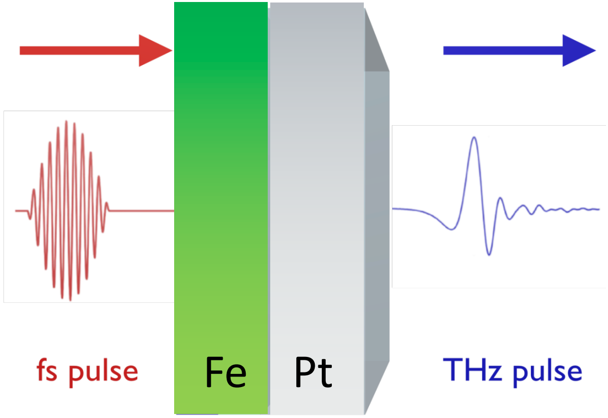

accelerated e$^-$ (transient current $\vec{j}_c$) emit THz-radiation

detected by standard THz time domain setup

T. Kampfrath *et al.*, Nat. Nanotechnol. **8**, 256 (2013)

Spin current ⟶ ISHE ⟶ electric current ⟶ THz

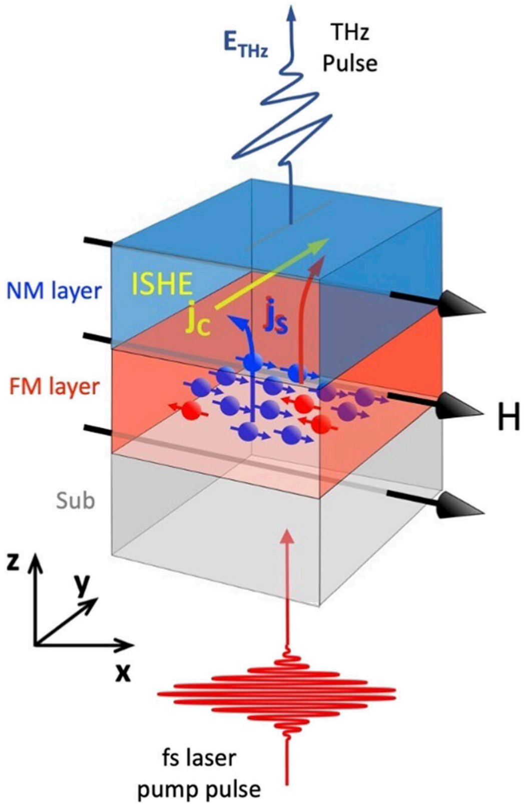

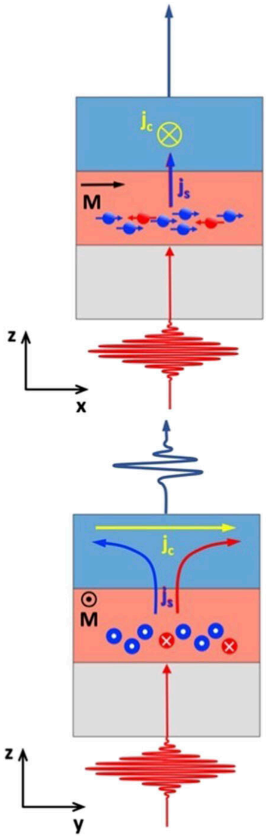

- e$^-$ diffuse in Pt layer
  $\mathbf{j_s}$ in both layers
- ISHE converts $\mathbf{j_s}$ into charge current $\mathbf{j_c}$ in Pt:

$$\vec{j}_c = \theta_{SH} \cdot \vec{j}_s \times \frac{\vec{M}}{|\vec{M}|}$$

- accelerated e$^-$ (transient current $\mathbf{j_c}$) emit THz-radiation
- detected by standard THz time domain setup

C. Bull et al., APL Materials 9, 090701 (2021)

Principle of THz generation

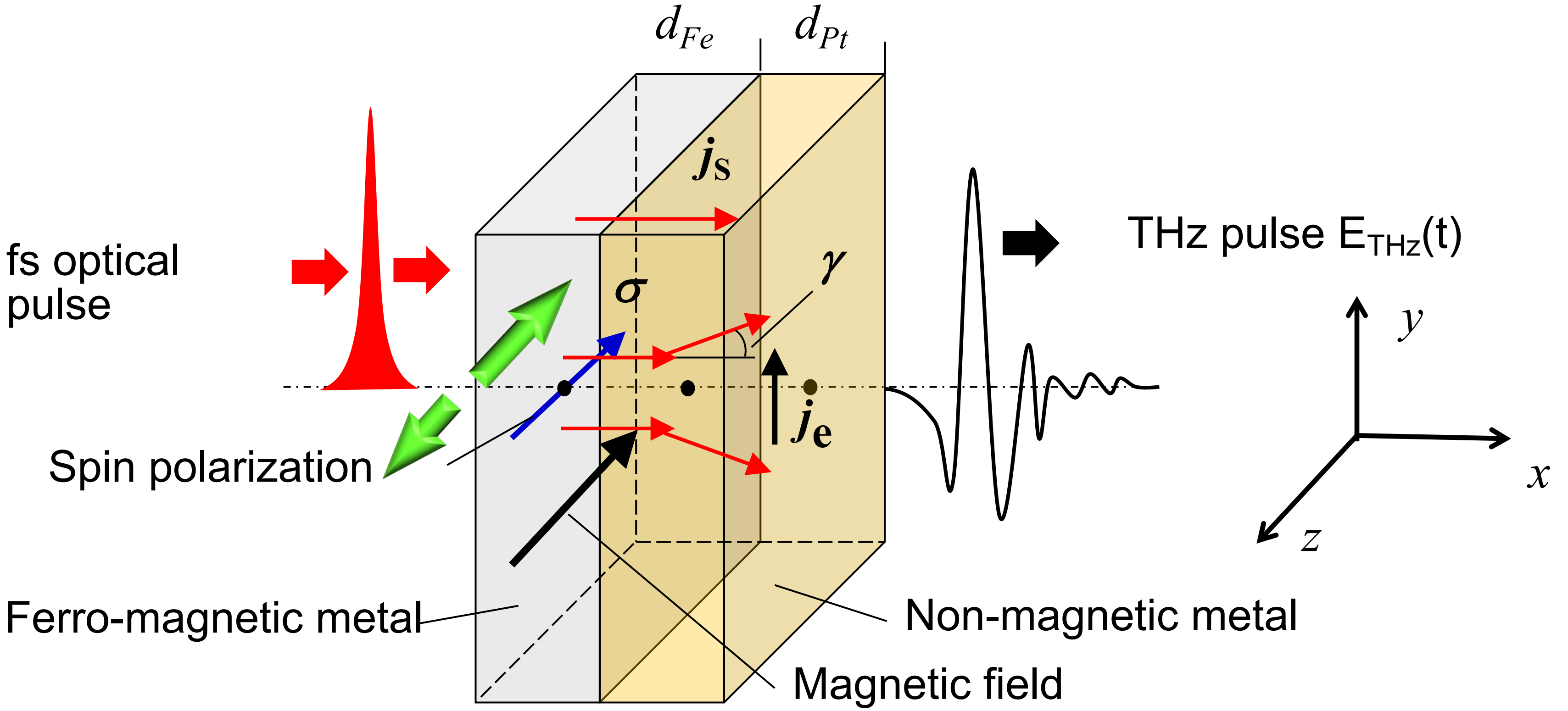

T. Seifert et al., Nature Photonics 10, 483 (2016) , Wu, Y. et al., Advanced Materials 29 ,1603031
Yang, D. et al., Advanced Optical Materials 4 , 1944–1949 (2016)

Efficient spintronic terahertz emitters:
Basic principles and technical realization

Content

- Introduction
- Femtosecond laser driven THz sources
- Spintronics and THz emission
- Technical realization
- Typical Results
- Outlook and Summary

Emitter design

Transmission geometry

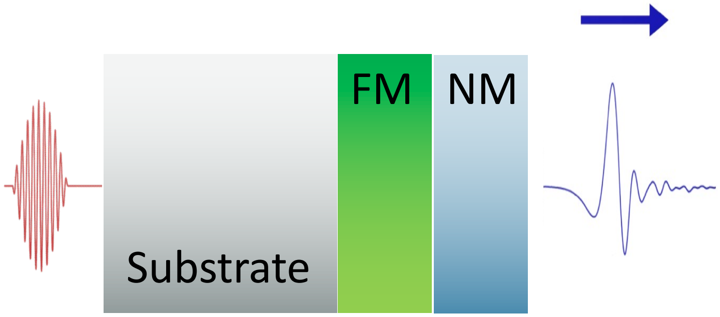

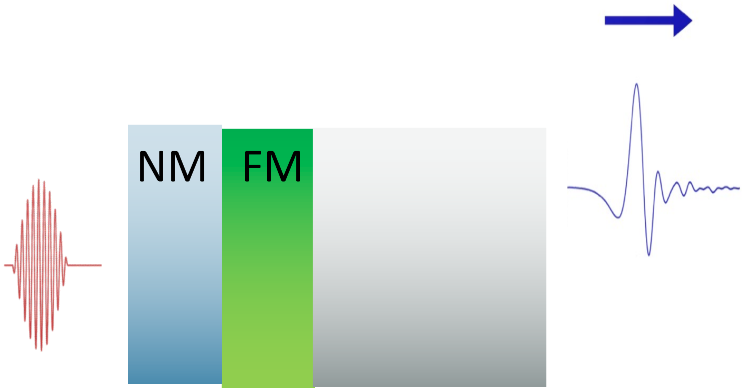

Substrate:	MgO, sapphire, semiconductor
Requirements:	transparent for pump light (and THz) non conducting lattice matched for epitaxial growth of Fe
Sequence of layers:	NM always top layer

Sequence of layers

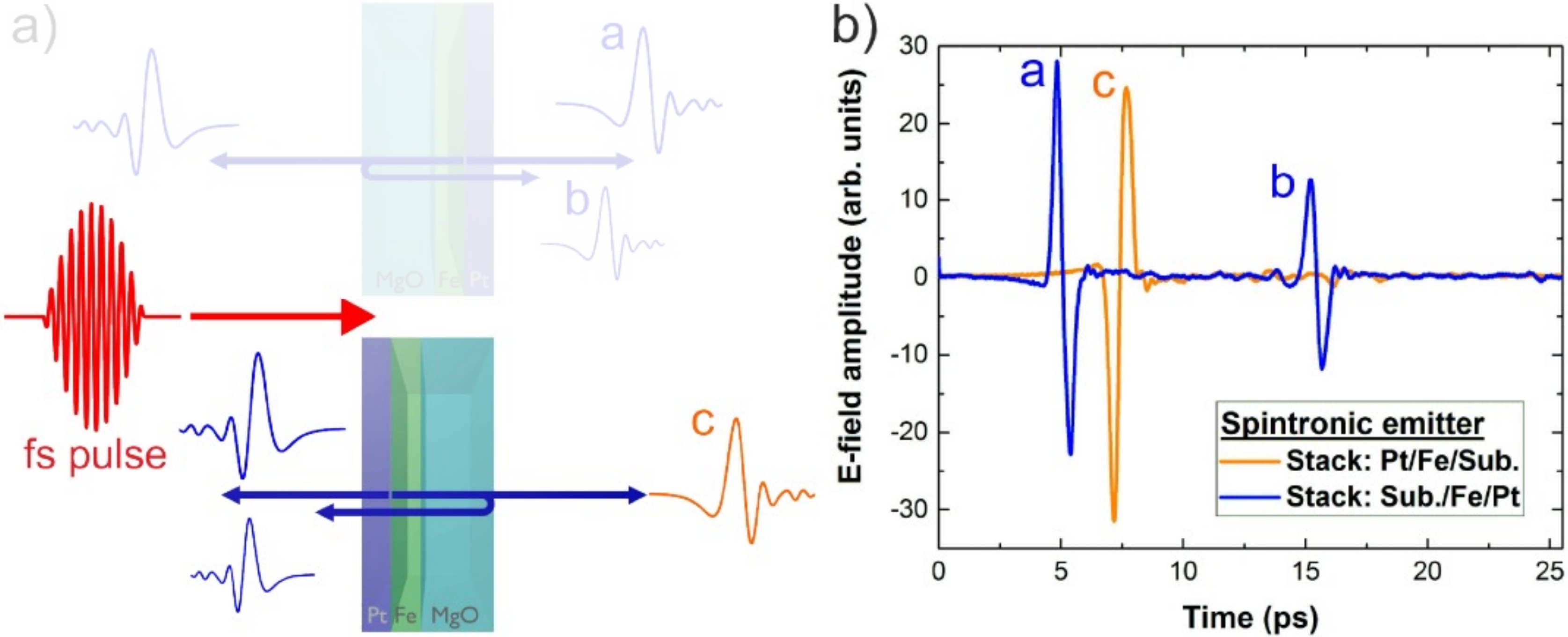

Optics

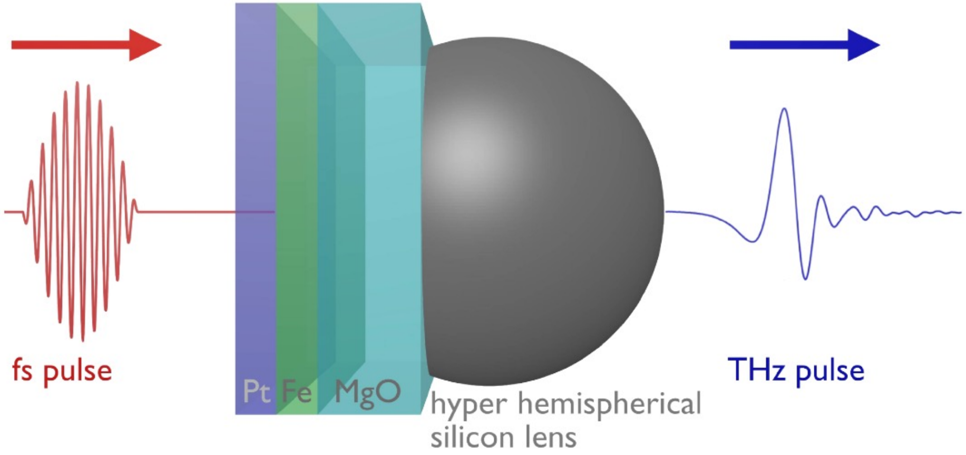

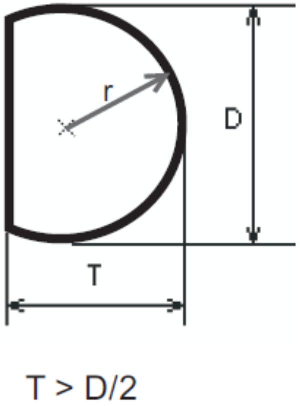

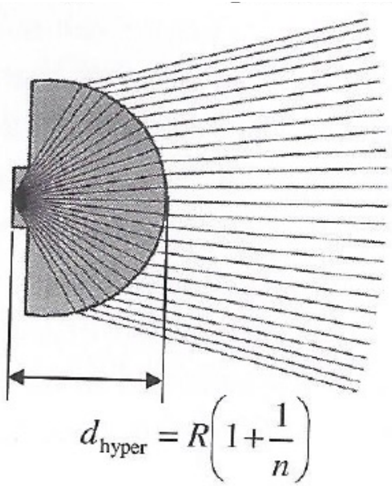

Small focus of pump beam leads to large divergence of THz beam

Collecting THz radiation with hyperhemispherical Si lens

G. Torosyan et al., Scientific Reports (2018) 8:1311

Hyperhemispherical Si lens

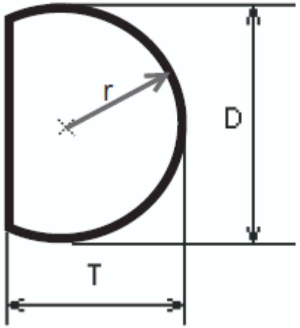

T > D/2

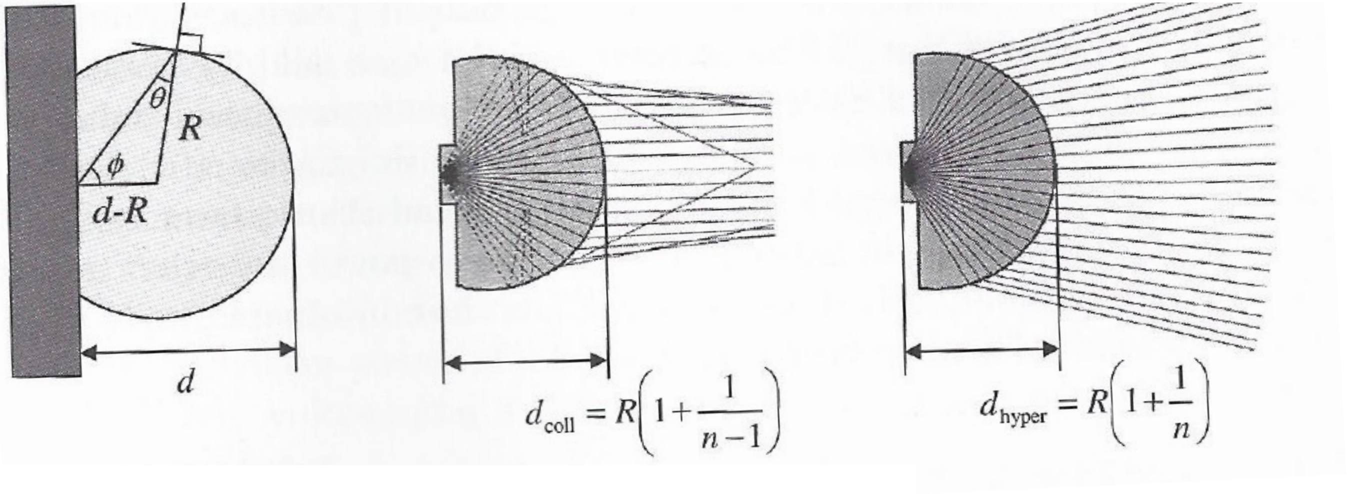

$$d_{\text{coll}} = R\left(1+\frac{1}{n-1}\right)$$

$$d_{\text{hyper}} = R\left(1+\frac{1}{n}\right)$$

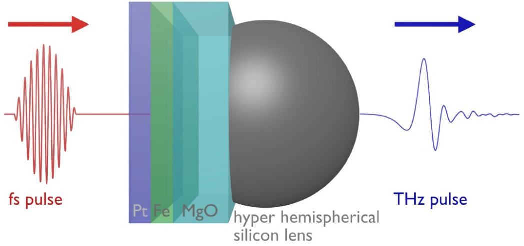

G. Torosyan et al., Scientific Reports (2018) 8:1311

Terahertz TDS system

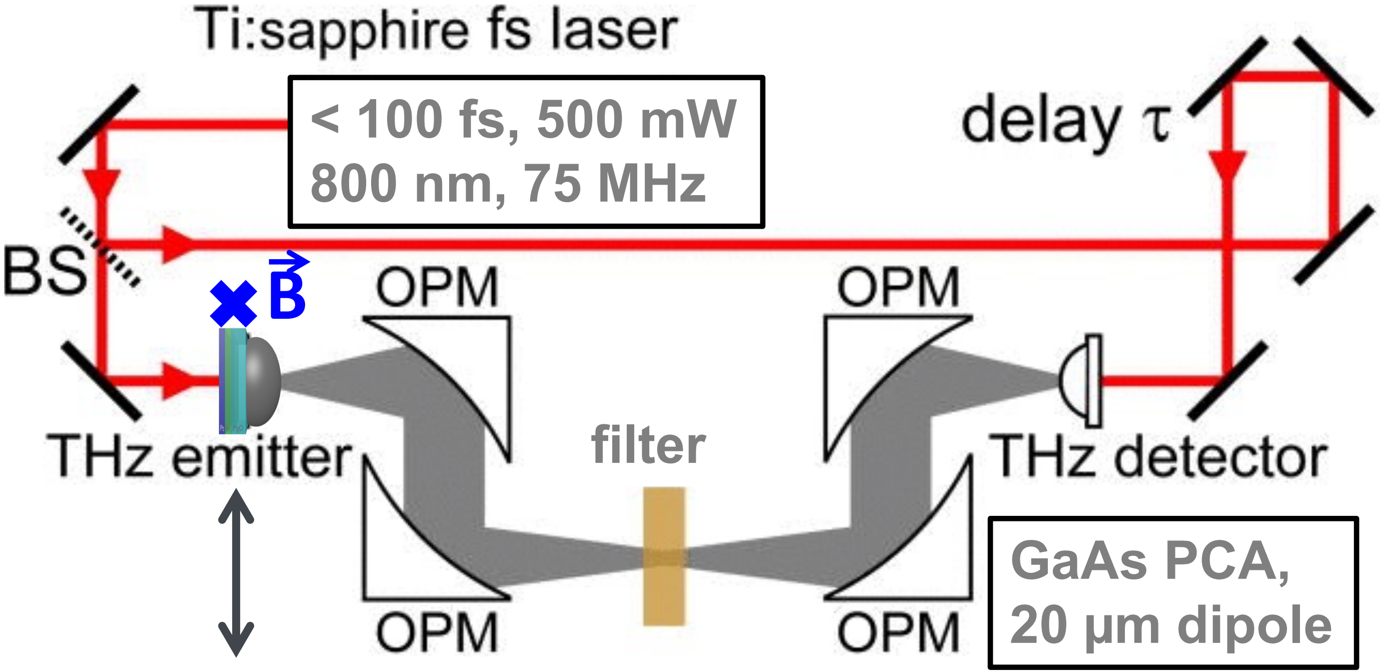

G. Torosyan et al., Scientific Reports (2018) 8:1311

Terahertz TDS system

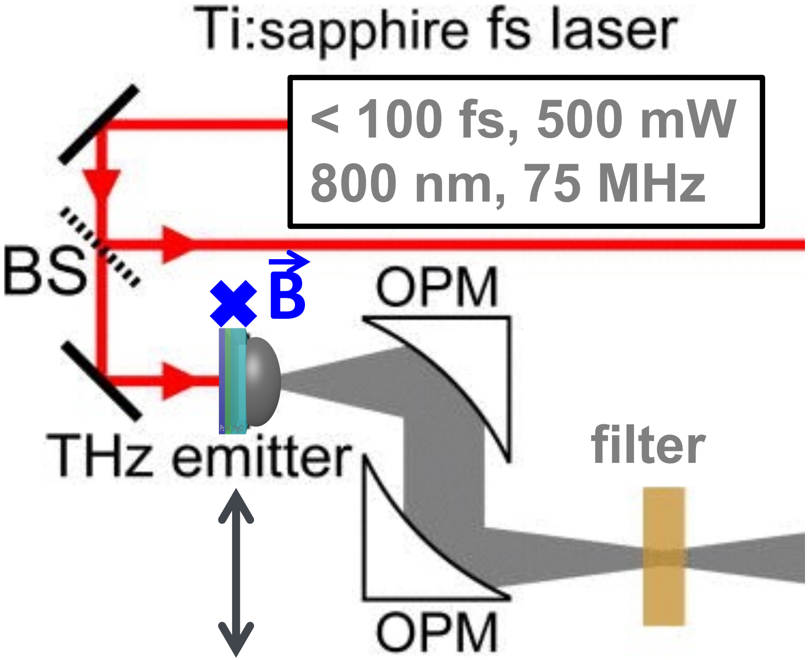

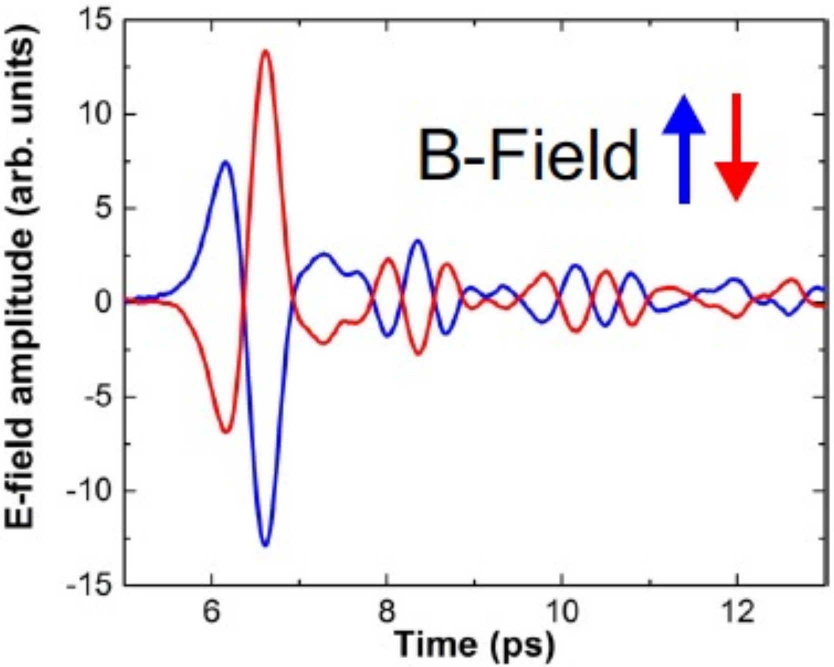

G. Torosyan et al., Scientific Reports (2018) 8:1311

Efficient spintronic terahertz emitters:

Basic principles and technical realization

Content

STE Optimization

Emitter design:	sequence of layers
	thickness
	multiple layers
	stacked emitters
	optics
Materials:	substrate
	nonmagnetic material
	ferromagnetic material
Layer fabrication:	epitaxial growth
	sputtering
Experimental set-up:	standard TDS system

Ferromagnet-metal-bilayer system

1. Ferromagnetic layer

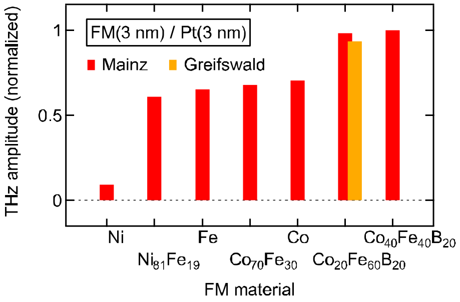

Co_{70} Fe_{60} B_{20}

Fe

Substrate and growth conditions ?

2. Non-magnetic layer

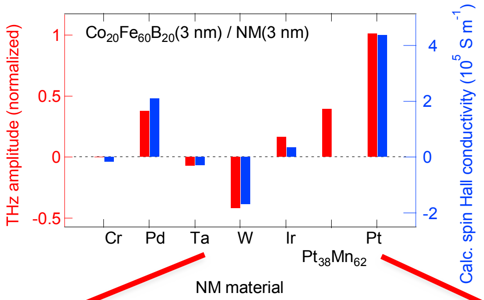

Pt

(W)

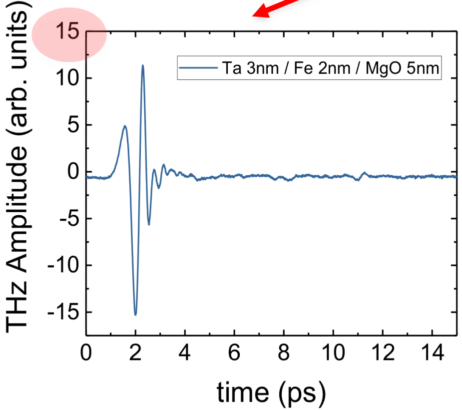

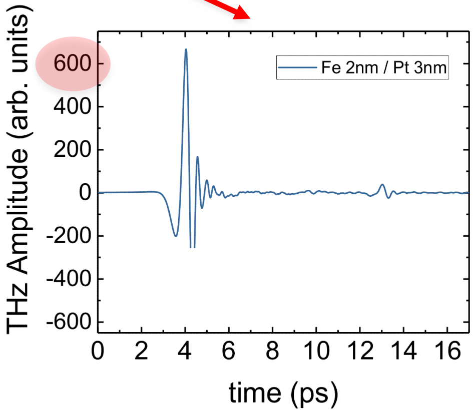

T. Seifert, *et.al.*, Nature Photonics, **10**, 483-488 (2016)

Substrates and growth conditions

Substrate materials:	MgO sapphire	Absortion in MgO above 3 THz reduces THz amplitude. Mismatch in sapphire lattice constants for Fe leads to high defect density . This may also influence the THz generation. In our experiments we have observed a weaker spectral amplitude at the maximum frequency whereas there is no obvious absorption at higher frequencies.
	Si GaAs	Generation of carriers in semiconductors leeds to THz absorption.

] T. Seifert, *et.al.*, Nature Photonics, **10**, 483-488 (2016)

Thin film growth

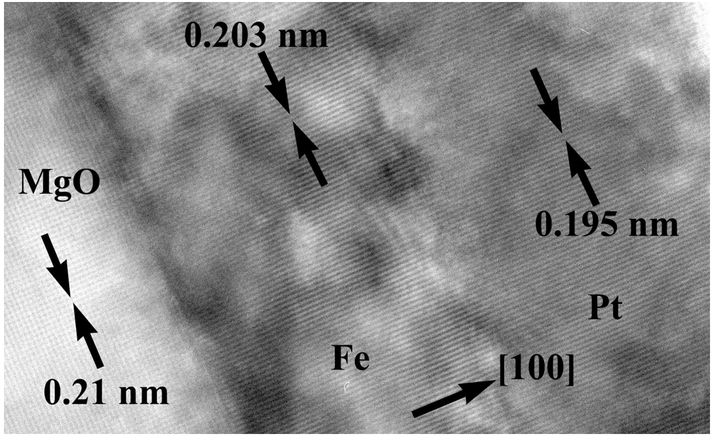

Fe/Pt layer system

Epitaxially grown on MgO (100) and Al_2O_3 (0001) substrates at 300 °C temperature.

Monitored in-situ by a calibrated quartz crystal oscillator

Characterized by:

X-ray reflectivity (XRR)
X-ray diffraction (XRD)
Transmission Electron Microscopy (TEM)

→ **High quality epitaxial bilayers**

E. Papaioannou et al., PRB 93, 134405 (2016)

Fe/Pt layer system

Epitaxial growth

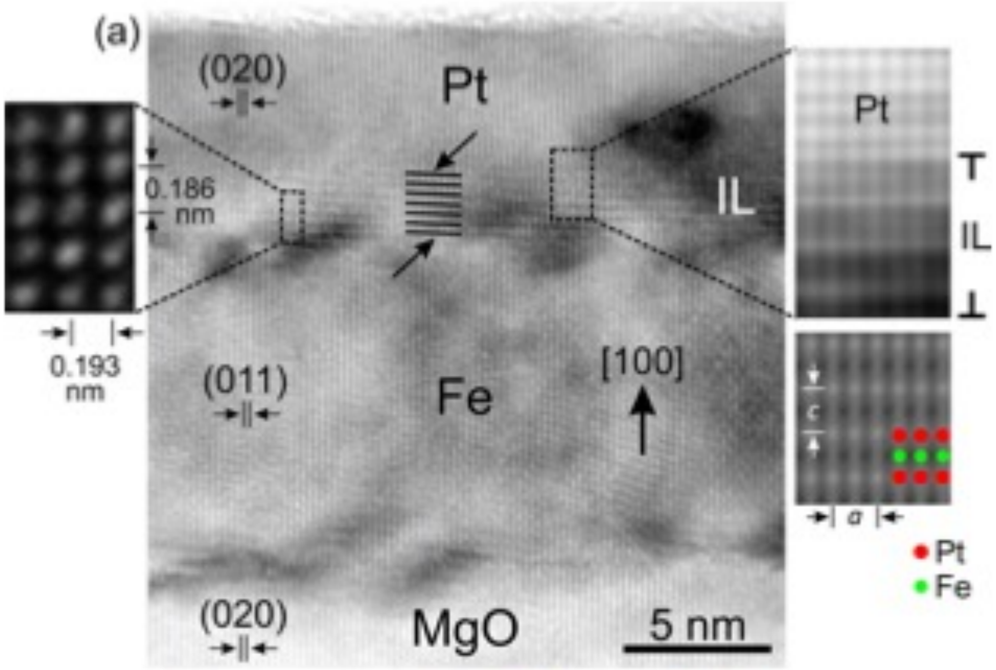

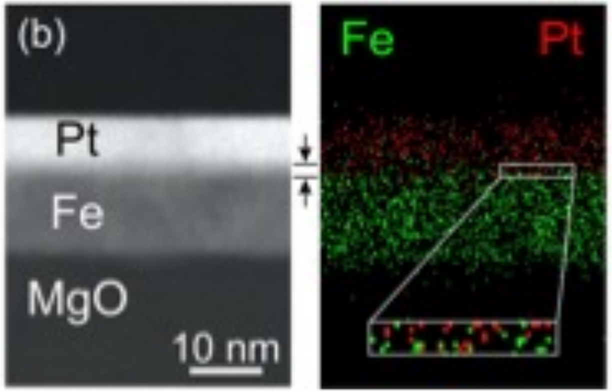

Fe/Pt alloy depending on growth temperature

E. Papaioannou et al., PRB 93, 134405 (2016)

Influence of the Crystal Structure

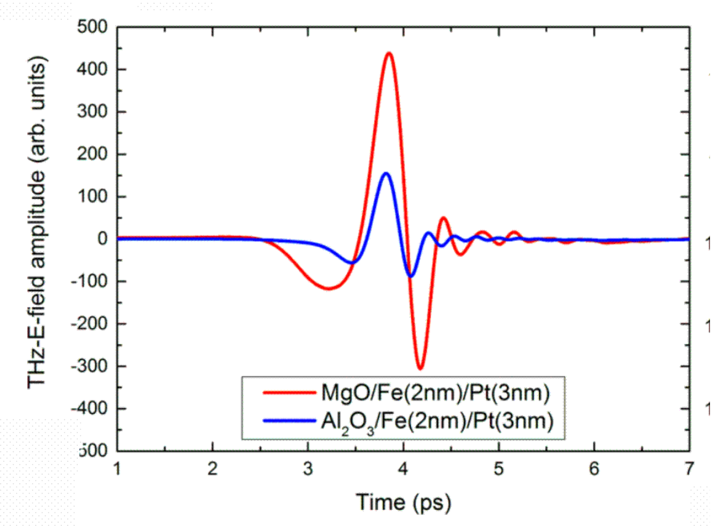

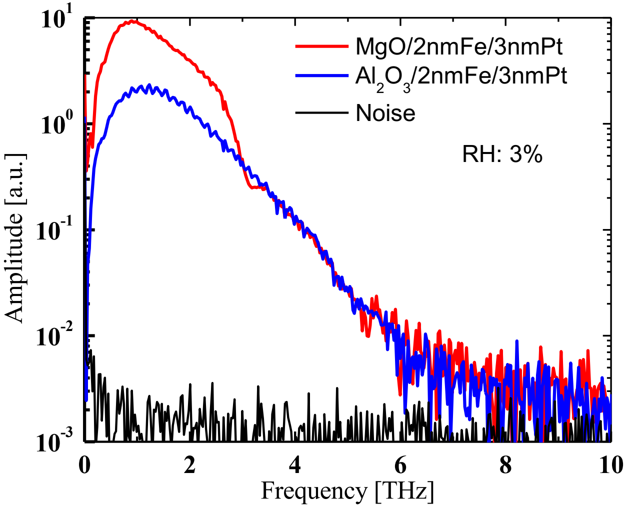

MgO substrate: Epitaxial growth of Fe and Pt: lower

Al_2O_3 substrate: Large lattice mismatch: higher

defect density

Polycrystalline growth of Fe and Pt

Influence of the Crystal Structure

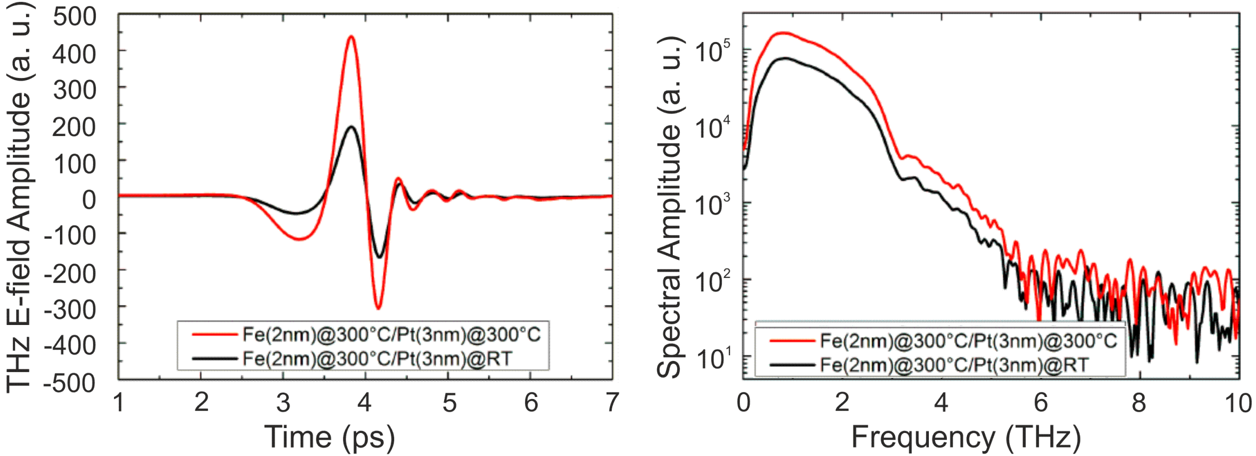

Fully epitaxial samples for growth temperatures of 300°C

Pt layers grown at RT display more defects

⇨ dropping THz E-field and spectral amplitude

pulse length and overall shape remains

Emitter geometries

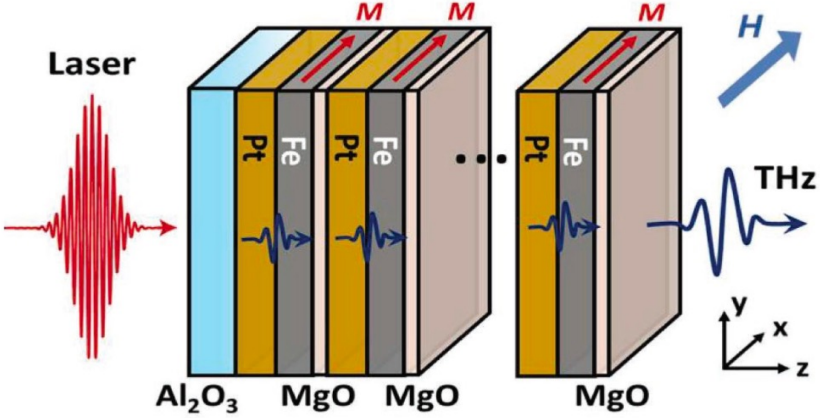

- Multiple emitters:
  Dielectric spacers
  Fe/Pt emitters

- Multilayers:
  One magnetic layer
  Two nonmagnetic layers

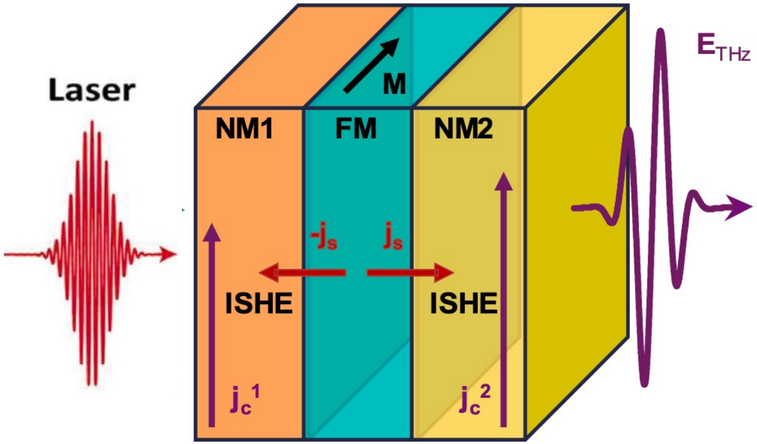

Multiple Emitters

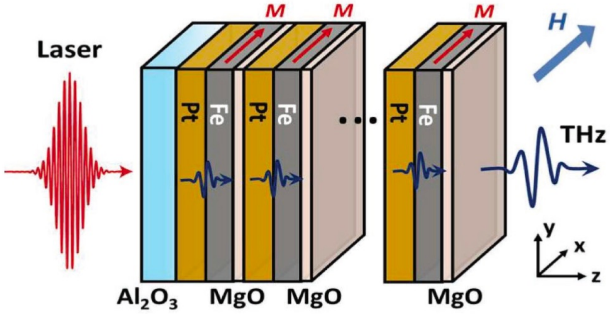

No spin currents through MgO

Additional absorption in metal layers

Number of stacks is limited

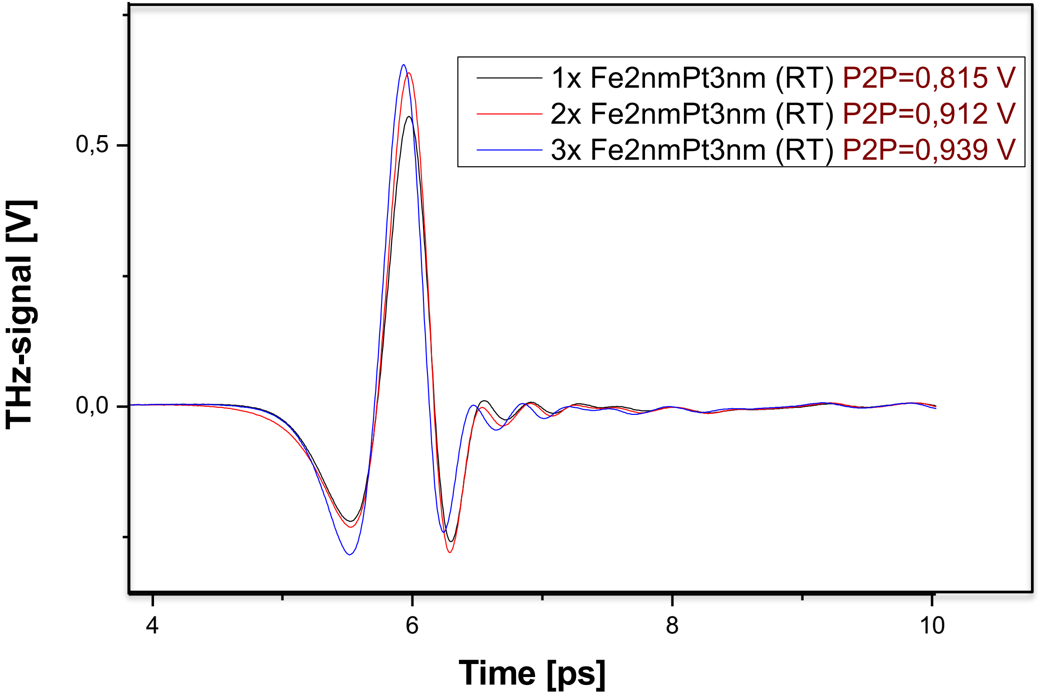

THz Generation in Multilayers

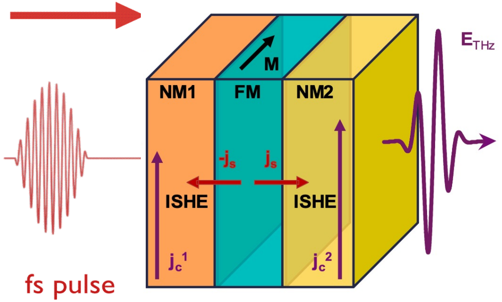

NM1 = NM2

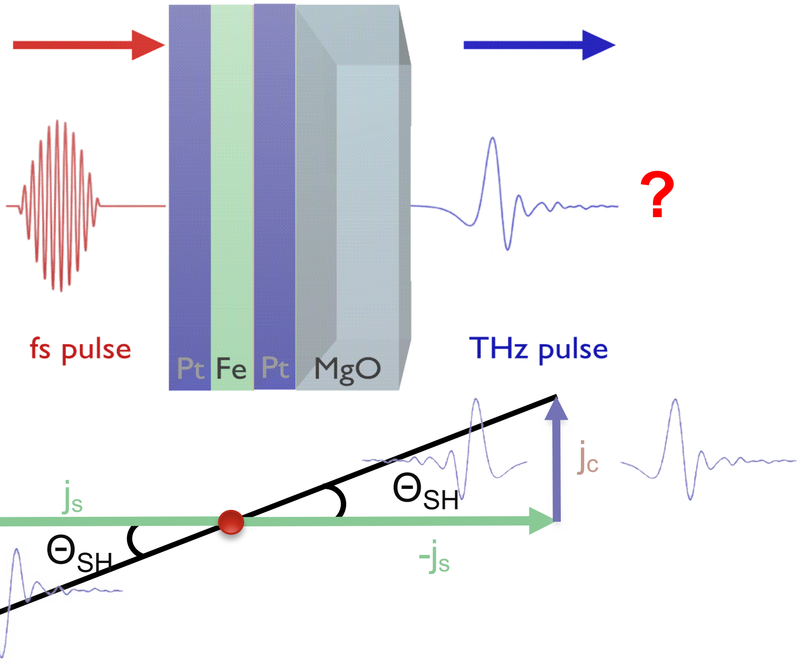

THz in forward direction generated from j_s and $-j_s$ cancel

THz Generation in Multilayers

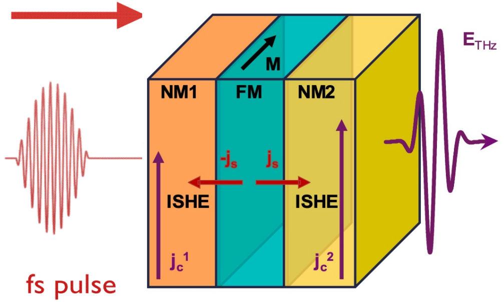

NM1 = NM2

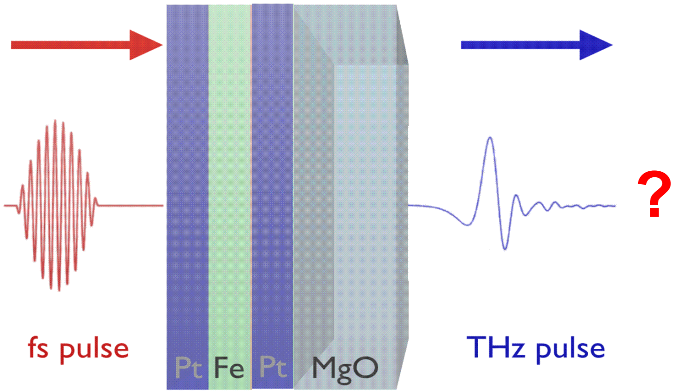

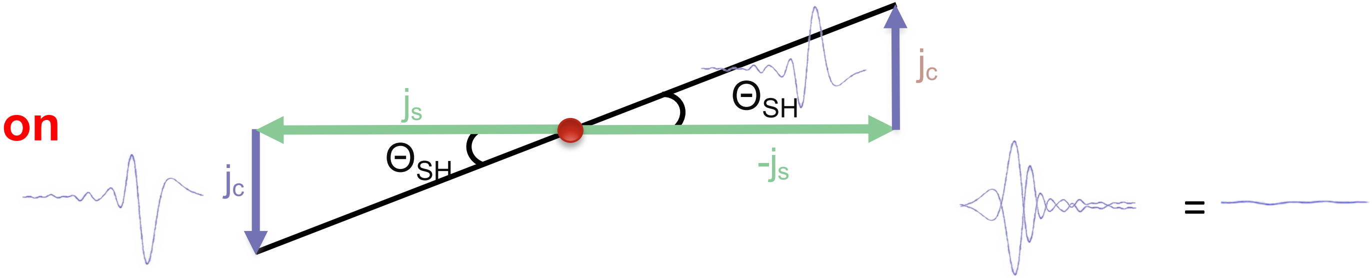

THz in forward direction generated from j_s and $-j_s$ cancel

THz Generation in Multilayers

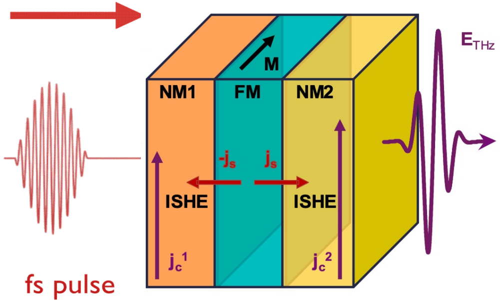

NM1 ≠ NM2

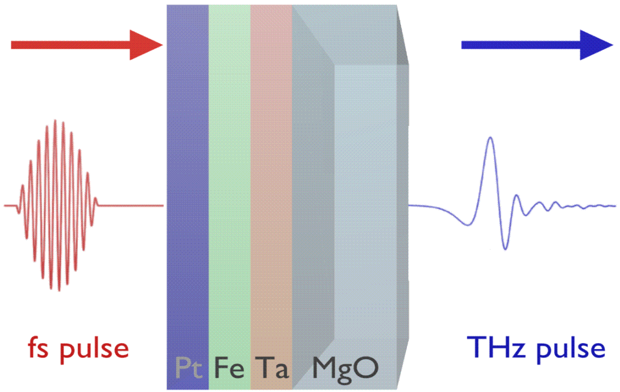

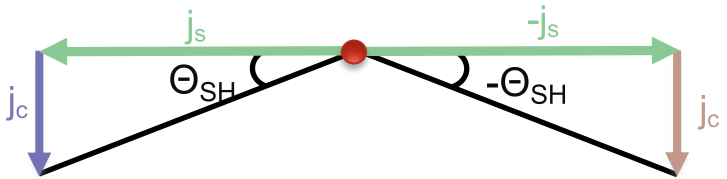

$$\theta_{SH1} \cdot \theta_{SH2} < 0$$

THz in forward direction generated from j_s and $-j_s$ add up

THz Generation in Multilayers

NM1 ≠ NM2

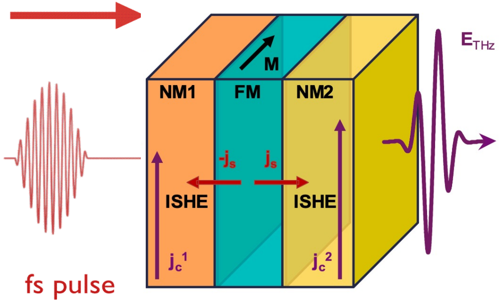

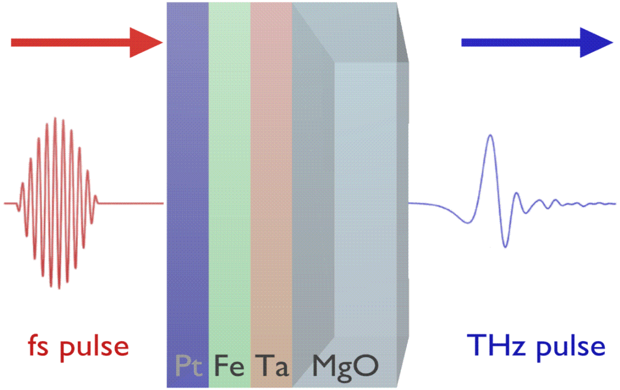

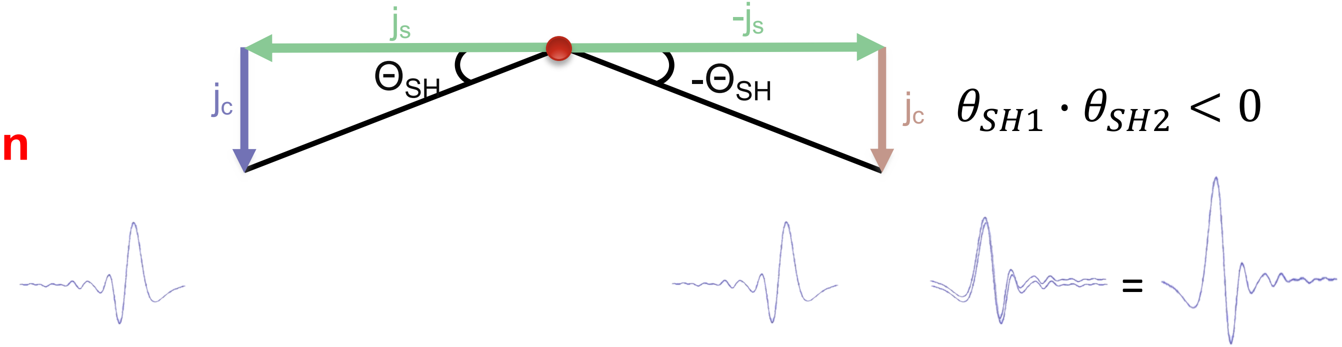

$\theta_{SH1} \cdot \theta_{SH2} < 0$

THz in forward direction generated from j_s and $-j_s$ add up

THz Emission from Multilayers

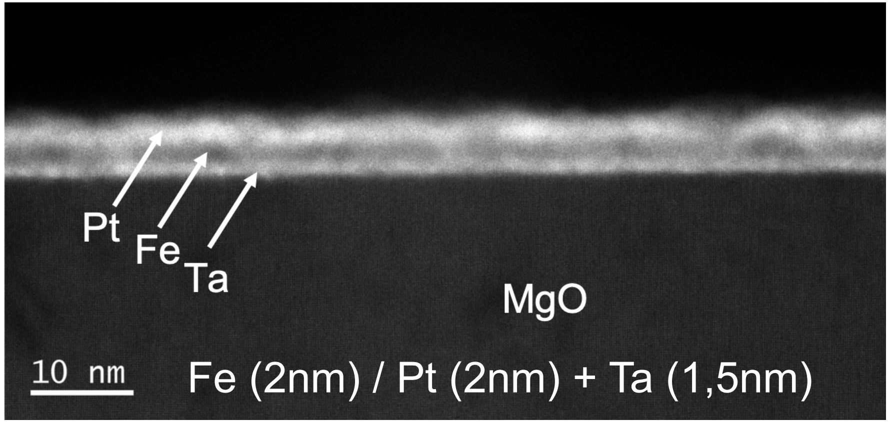

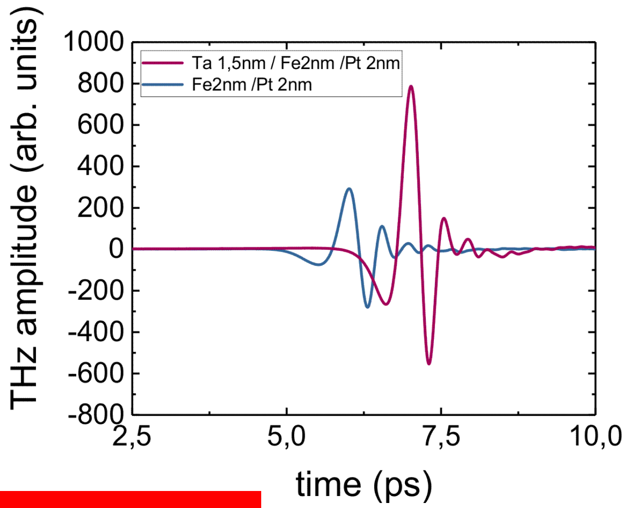

Optimum 3-layer structure:
W(3 nm)/$Co_{40}Fe_{40}B_{20}$(2 nm)/Pt(3 nm)

Thickness dependence

Qualitative considerations

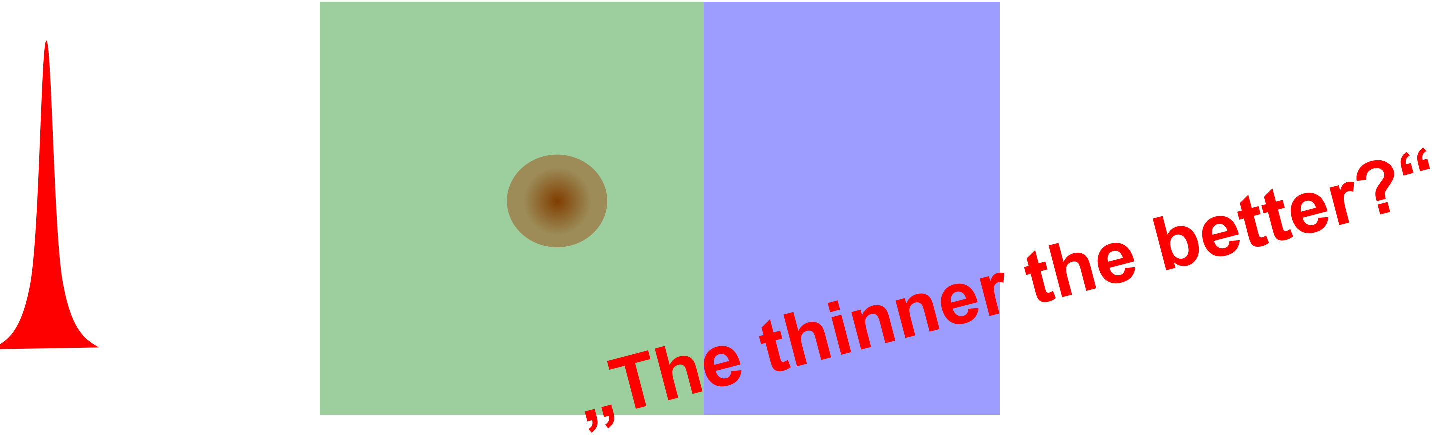

- diffusion in Fe restricts the excitation region
- limited close to boundary

- diffusion in Pt restricts Pt thickness
- thickness ≈ diffusion length

Thickness dependence

Pt thickness

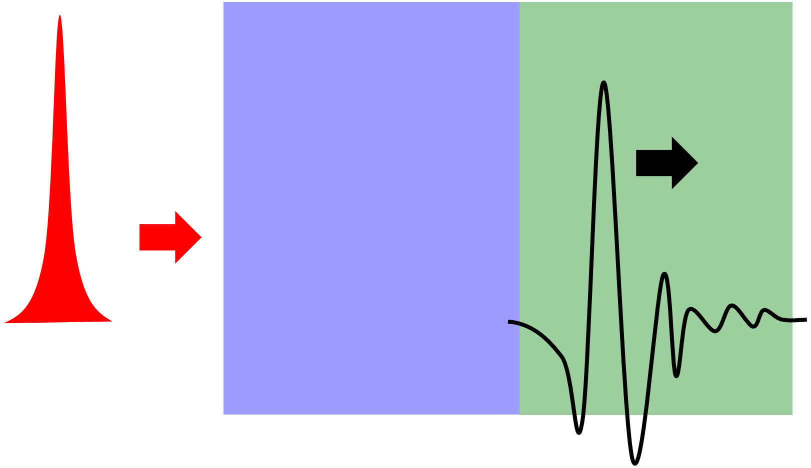

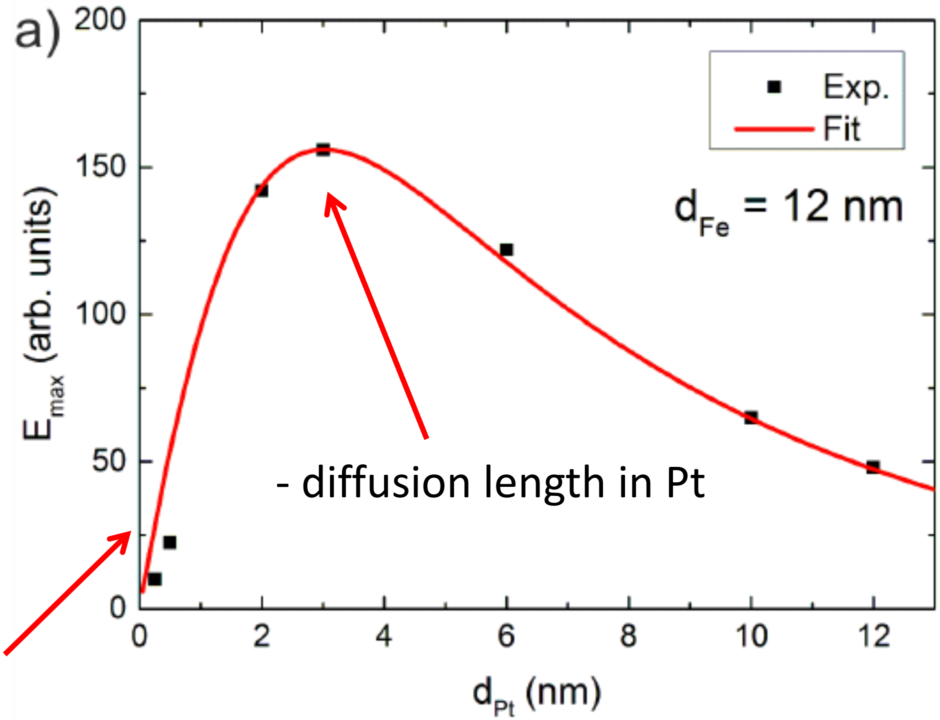

- diffusion length in Pt

- small current
- high resistivity

Thickness dependence

Fe thickness

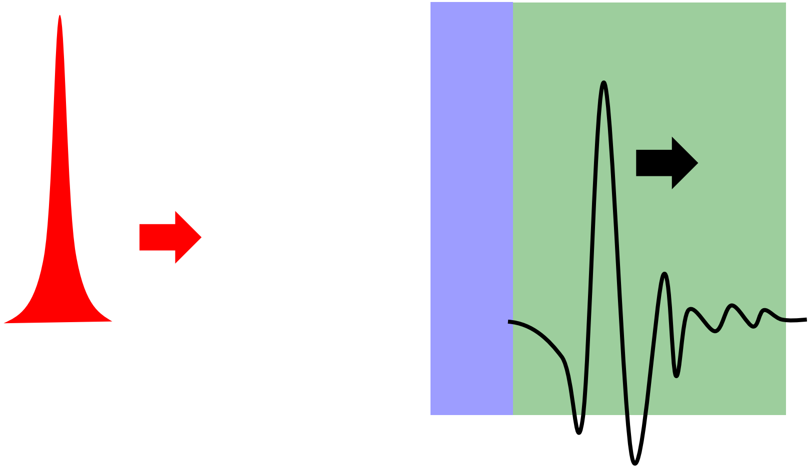

- reduced number of spin polarized electrons
- no magnetic poperties

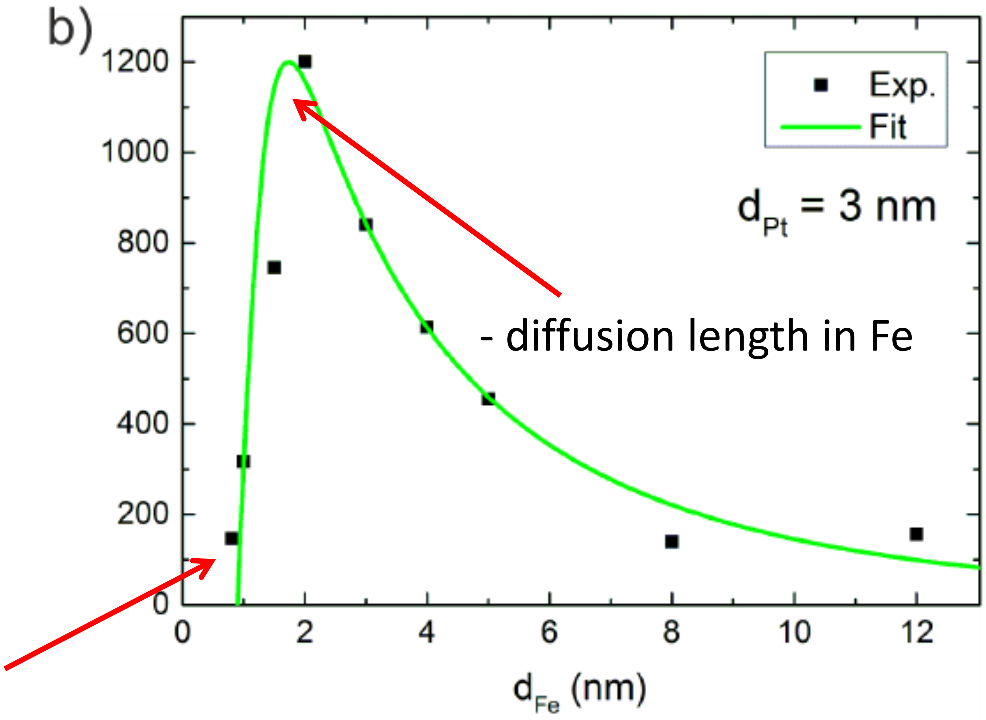

- diffusion length in Fe

G. Torosyan et al., Scientific Reports (2018) 8:1311

Thickness dependence

Processes considered in our model:

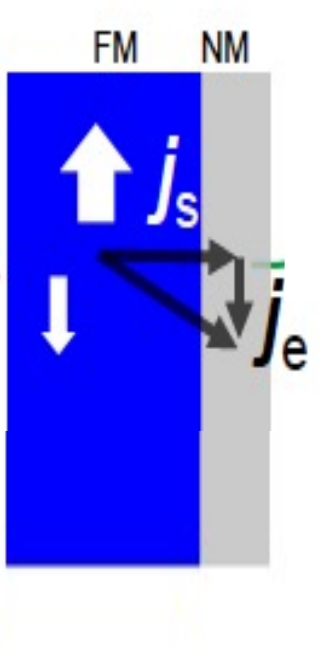

1. Generation of spin polarization j_S

2. Spin diffusion and accumulation in Fe and Pt $j_C = \gamma\, j_S$

3. Electrical and optical properties in the bilayer $Z = Z(\omega),\ n$

4. Absorption of THz radiation $k^* = \dfrac{n^*\omega}{c} = \dfrac{n_{metal}\omega}{c} - i\dfrac{\kappa\omega}{c}$

Theoretical considerations

Wave equation in the frequency domain: $[\partial_z^2 + k^2(z,\omega)]\boldsymbol{E}(z,\omega) = Z_0\omega\,\boldsymbol{j}_c(z,\omega)/ic$

Green‘s function approach (Sipe, J.E., New Green-function formalism for surface optics. *J. Opt. Soc.***4**, 481 (1987)):

e

$$E_{THz}(\omega) = Z(\omega)e\int_0^d j_C dz = Z(\omega)e\int_0^d \gamma(z)\, j_S(z,\omega)dz$$

No phase changes during propagation in metal layers and weak absorption in the metal layers:

$$\left|e^{-ikz}\right| = 1 \qquad k = \frac{n\omega}{c} \rightarrow k^* = \frac{n^*\omega}{c} = \frac{n_{metal}\omega}{c} - i\frac{\kappa\omega}{c}$$

T. Kampfrath et al., Nature Nanotechnology **8**, 256 (2013)

Simulation

$$E_{\mathrm{THz}} \propto \frac{P_{\mathrm{abs}}}{d_{\mathrm{Fe}}+d_{\mathrm{Pt}}} \cdot \tanh\left(\frac{d_{\mathrm{Fe}}-d_0}{2\lambda_{\mathrm{pol}}}\right) \cdot \frac{1}{n_{\mathrm{air}}+n_{\mathrm{MgO}}+Z_0\cdot(\sigma_{\mathrm{Fe}}d_{\mathrm{Fe}}+\sigma_{\mathrm{Pt}}d_{\mathrm{Pt}})} \cdot \tanh\left(\frac{d_{\mathrm{Pt}}}{2\lambda_{\mathrm{Pt}}}\right) \cdot e^{-(d_{\mathrm{Fe}}+d_{\mathrm{Pt}})/s_{\mathrm{THz}}}$$

„useful“ pump light absorption

generation of spin polarized electrons

generation of charge current via ISHE

absorption losses in metal layers

G. Torosyan et al., Scientific Reports (2018) 8:1311

Simulation

$$E_{\mathrm{THz}} \propto \frac{P_{\mathrm{abs}}}{d_{\mathrm{Fe}}+d_{\mathrm{Pt}}} \cdot \tanh\left(\frac{d_{\mathrm{Fe}}-d_0}{2\lambda_{\mathrm{pol}}}\right) \cdot \frac{1}{n_{\mathrm{air}}+n_{\mathrm{MgO}}+Z_0\cdot(\sigma_{\mathrm{Fe}}d_{\mathrm{Fe}}+\sigma_{\mathrm{Pt}}d_{\mathrm{Pt}})} \cdot \tanh\left(\frac{d_{\mathrm{Pt}}}{2\lambda_{\mathrm{Pt}}}\right) \cdot e^{-(d_{\mathrm{Fe}}+d_{\mathrm{Pt}})/s_{\mathrm{THz}}}$$

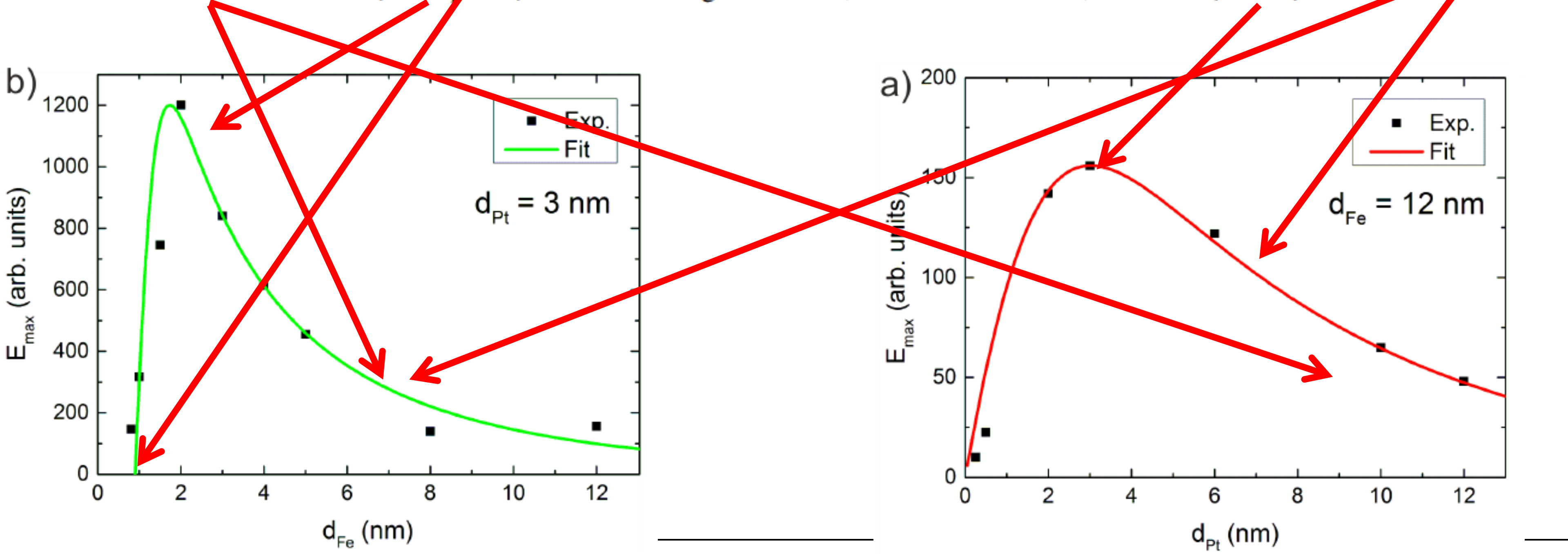

G. Torosyan et al., Scientific Reports (2018) 8:1311

Simulation

$$E_{\mathrm{THz}} \propto \frac{P_{\mathrm{abs}}}{d_{\mathrm{Fe}}+d_{\mathrm{Pt}}} \cdot \tanh\left(\frac{d_{\mathrm{Fe}}-d_0}{2\lambda_{\mathrm{pol}}}\right) \cdot \frac{1}{n_{\mathrm{air}}+n_{\mathrm{MgO}}+Z_0\cdot(\sigma_{\mathrm{Fe}}d_{\mathrm{F}}} \cdot \tanh\left(\frac{d_{\mathrm{Pt}}}{}\right) \cdot e^{-(d_{\mathrm{Fe}}+d_{\mathrm{Pt}})/s_{\mathrm{THz}}}$$

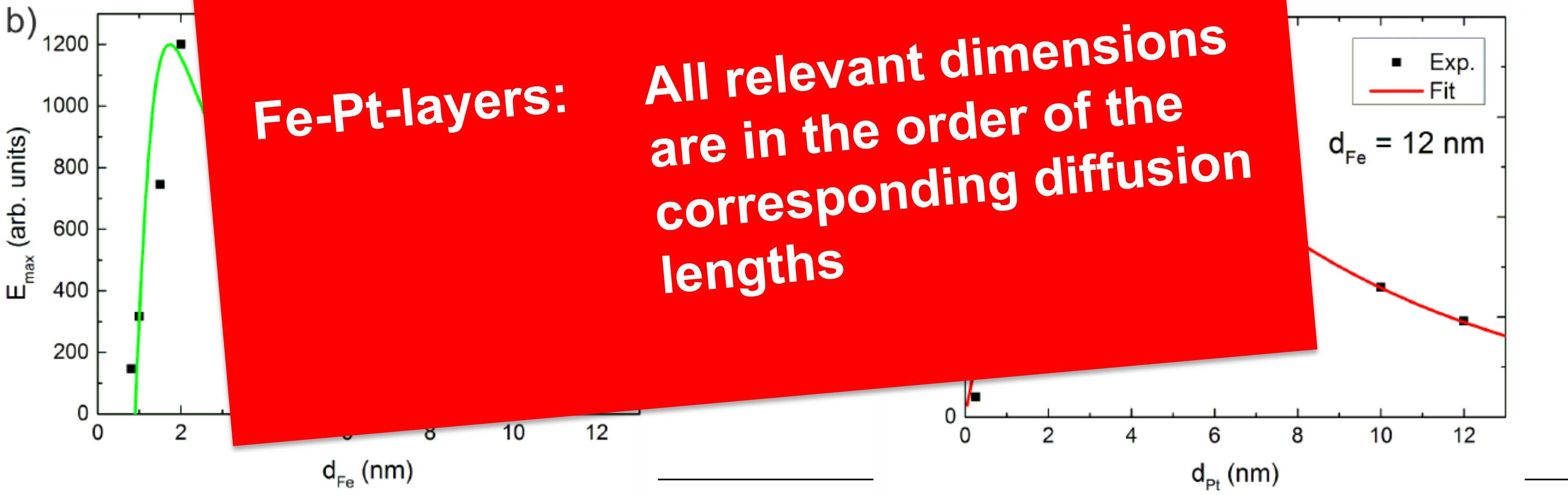

Fe-Pt-layers:

All relevant dimensions are in the order of the corresponding diffusion lengths

G. Torosyan et al., Scientific Reports (2018) 8:1311

Power dependence

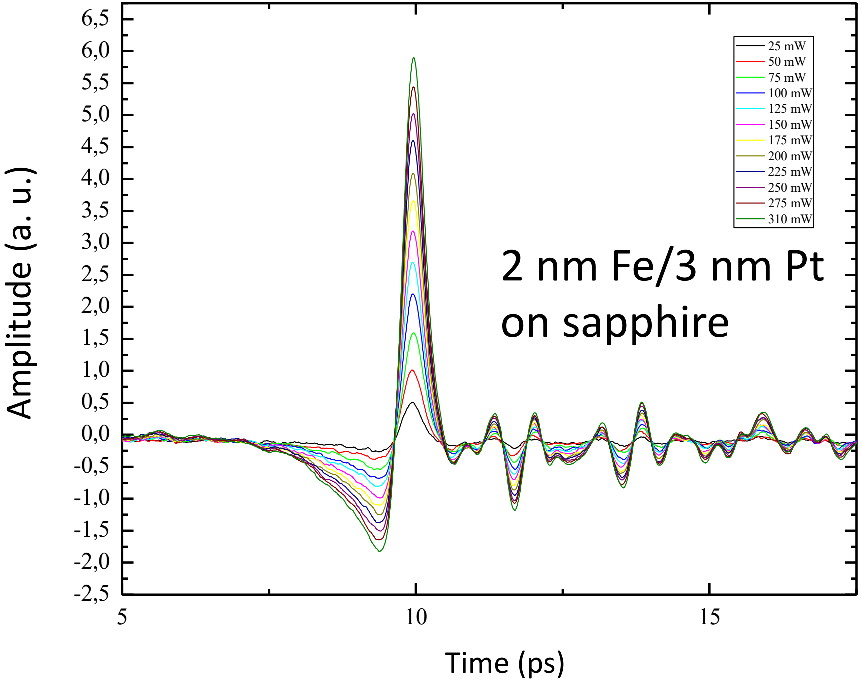

2 nm Fe/3 nm Pt
on sapphire

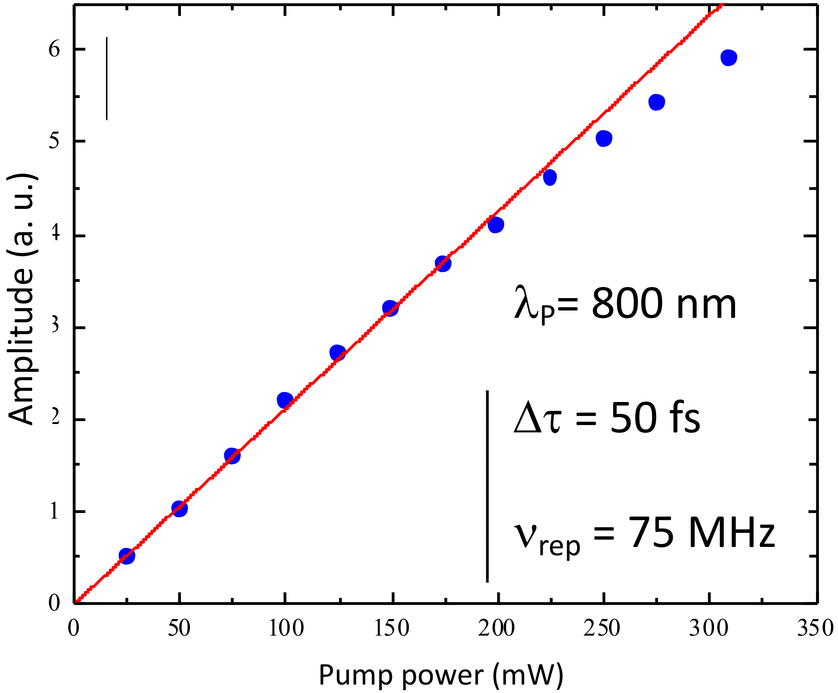

λ_P= 800 nm

$\Delta\tau$ = 50 fs

ν_{rep} = 75 MHz

G. Torosyan et al., Scientific Reports (2018) 8:1311

Pulse length

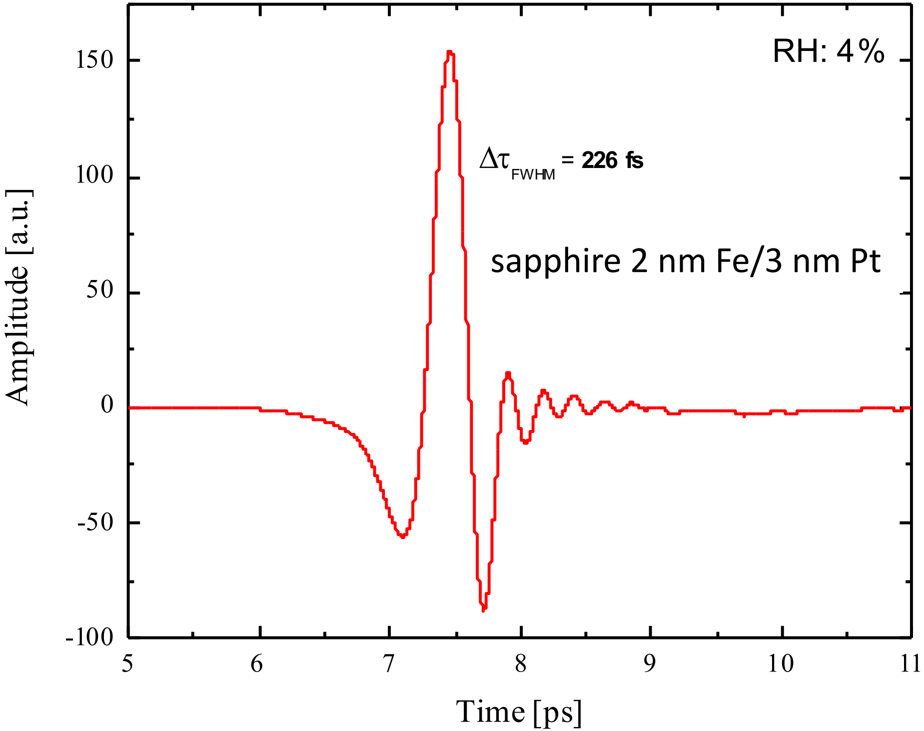

- pulse length < 250 fs
- limited by pump pulse length
- strong oscillations
- shorter pulses for sapphire substrate

G. Torosyan et al., Scientific Reports (2018) 8:1311

Bandwidth

3 nm Fe/3 nm Pt on sapphire

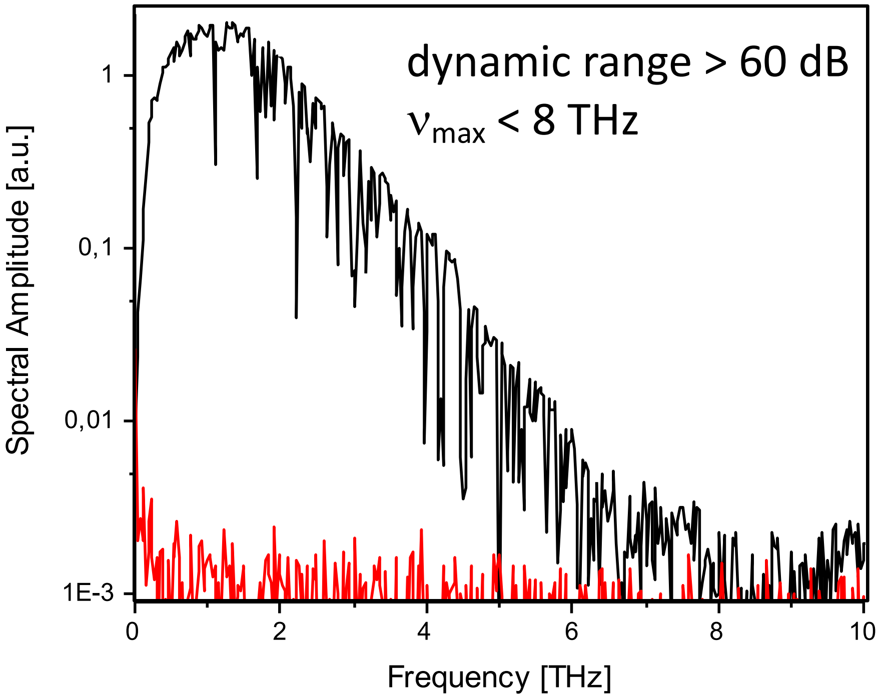
dynamic range > 60 dB

ν_{max} < 8 THz

Substrate:

MgO

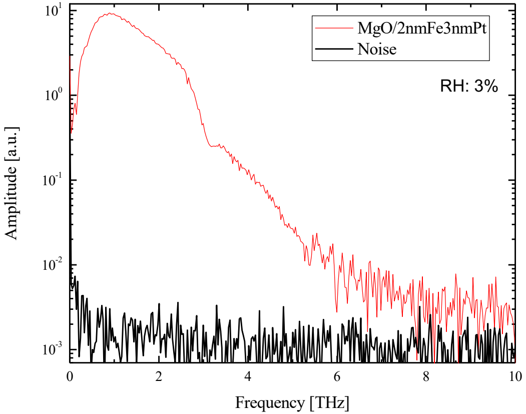

sapphire

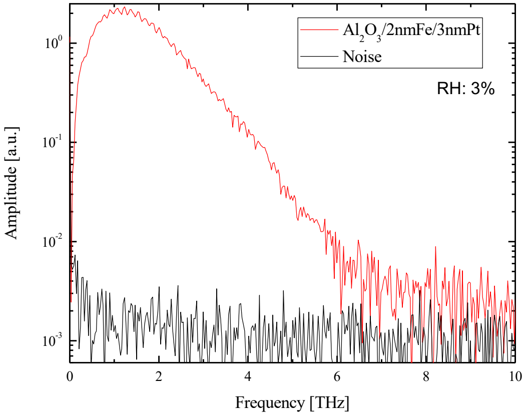

G. Torosyan et al., Scientific Reports (2018) 8:1311

Bandwidth

3 nm Fe/3 nm Pt on sapphire

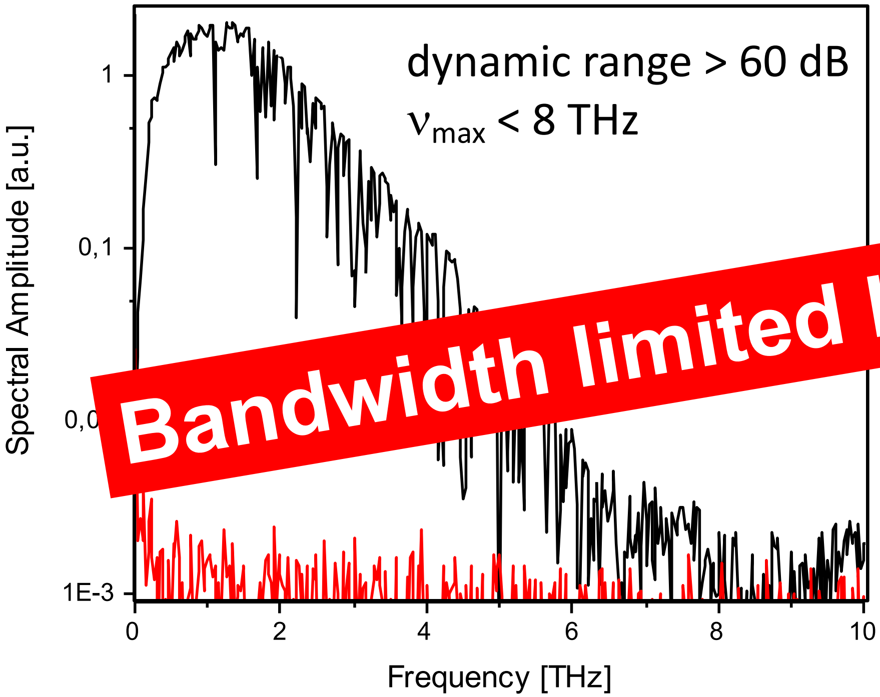
dynamic range > 60 dB

ν_{max} < 8 THz

Bandwidth limited by detector

Substrate:

MgO

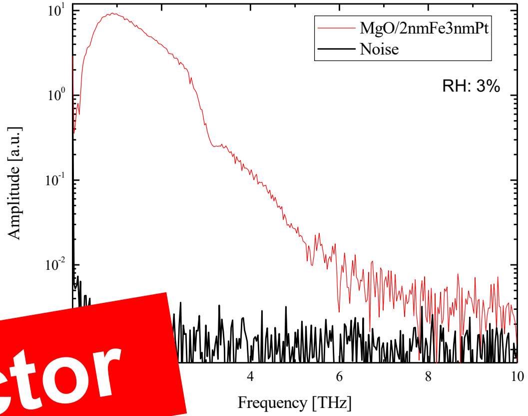

sapphire

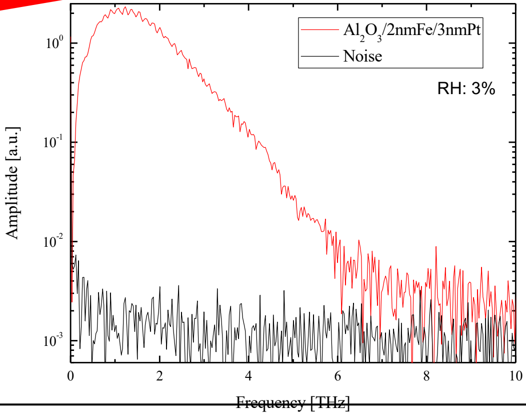

G. Torosyan et al., Scientific Reports (2018) 8:1311

Bandwidth

Photoconductive switch

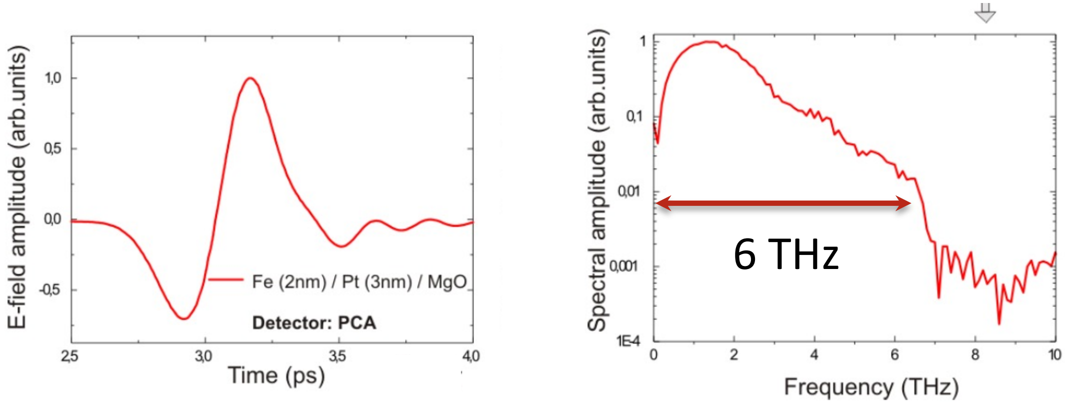

Electro-optical sampling

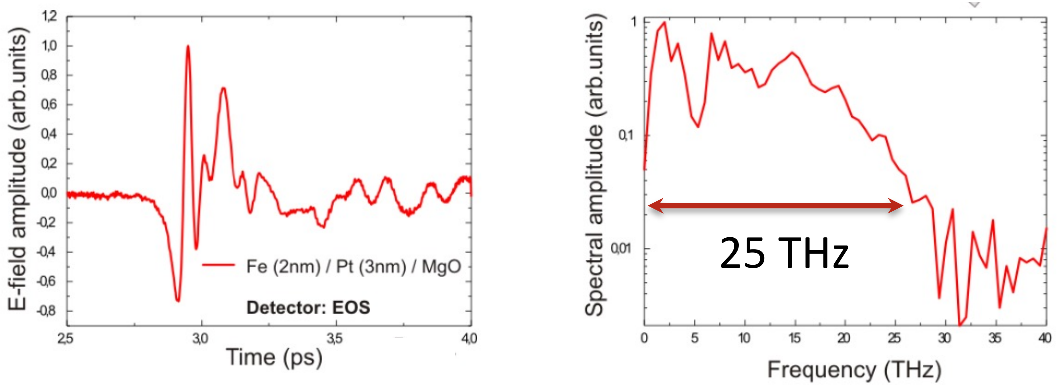

Bandwidth

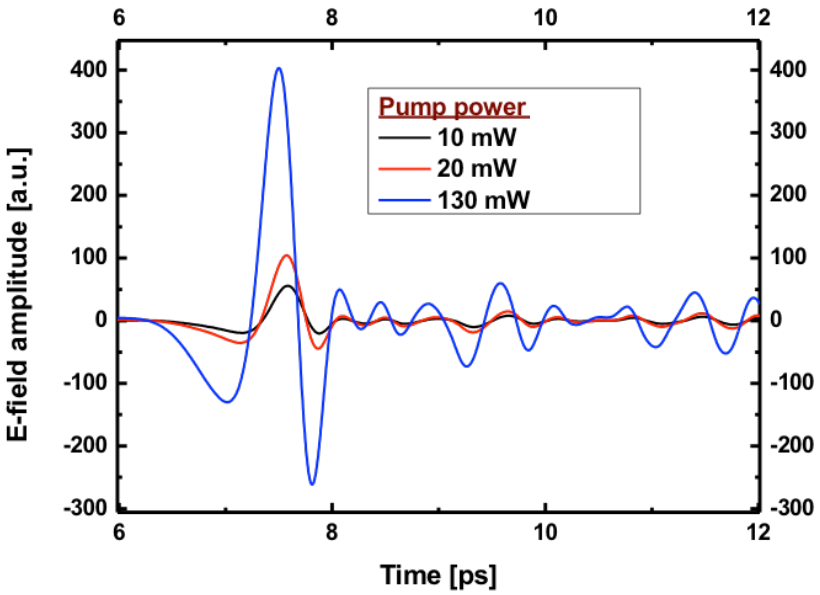

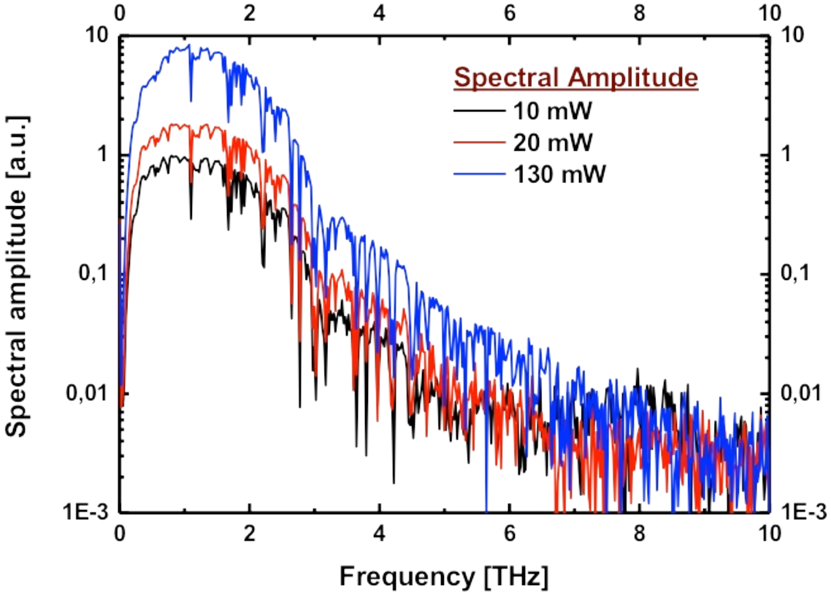

- usefull THz signal for pump powers < 10 mW
- dynamic range > 40 dB even for very low pump power

G. Torosyan et al., Scientific Reports (2018) 8:1311

Pump wavelength dependence

Pump photons excite spin polarized electrons

Excitation depends on bandstructure

In principle no threshold (no bandgap)

however

energy dependent spin transport and filtering at the Fe-Pt-boundary result in photon energy threshold

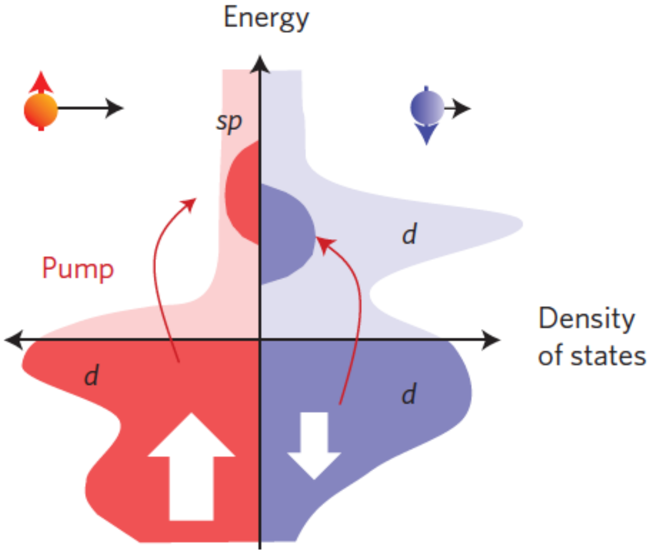

→ 1.55 µm fiber laser as convenient pump source?

Wavelength dependence

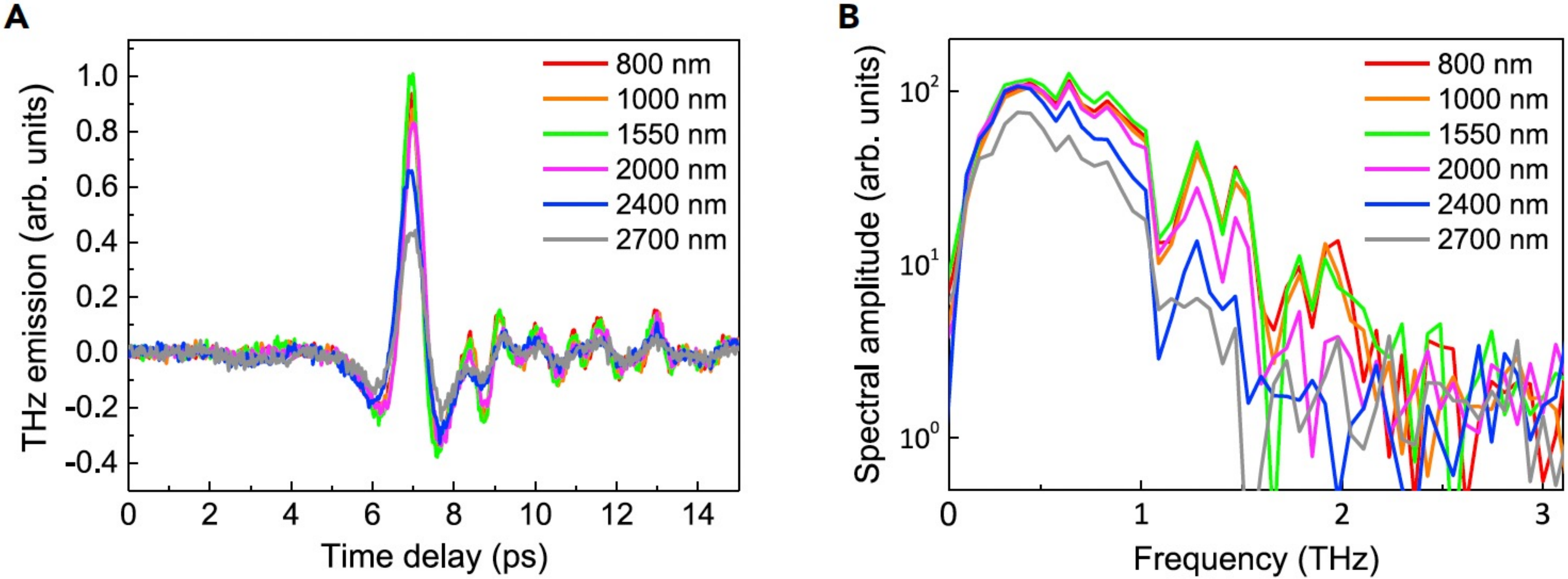

Wavelength dependence

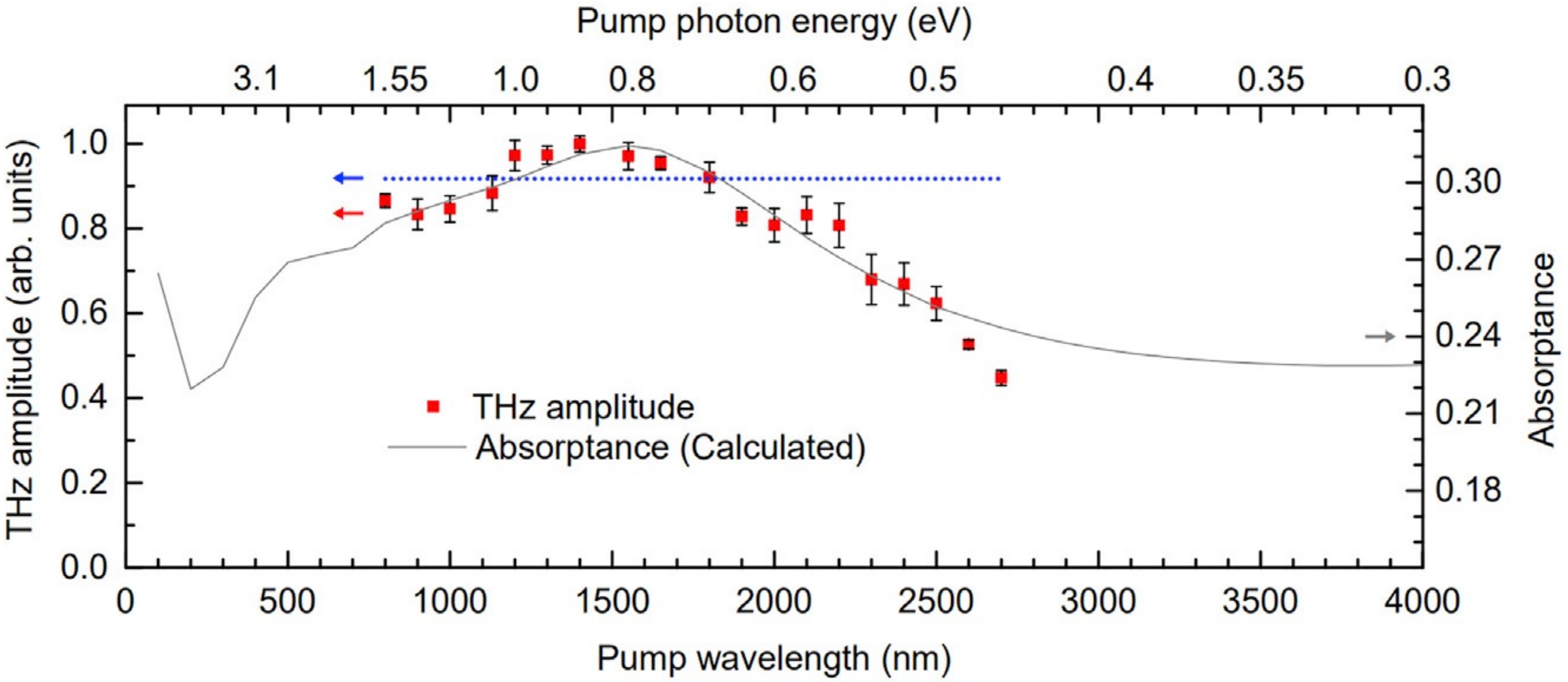

Wavelength dependence

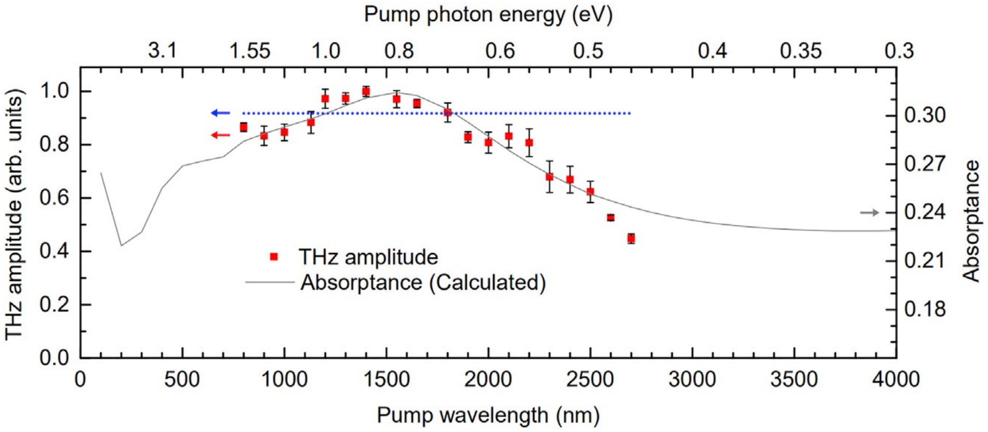

Ultrashort fiber laser at 1.5 µm

THz emission from STE is almost wavelength independent

„Maximum“ between 1200 nm and 1800 nm

Energy dependent spin transport and filtering at the Fe-Pt-boundary

→ photon energy threshold around 0.35 eV (3.5 µm)

1.5 µm - 800 nm comparison

Equal effective as a THz radiation source when excited either at **λ = 800 nm** or at **λ = 1550 nm**

Efficient radiation even with low incident power levels

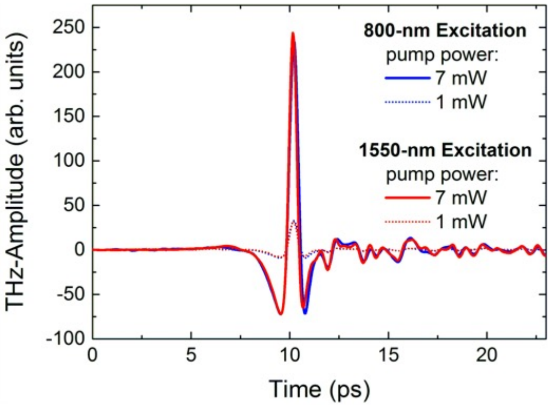

Integration of spintronic emitters in THz systems driven by relatively low cost and compact fs fiber lasers without the need for frequency conversion

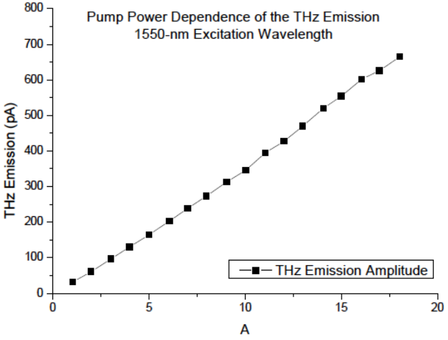

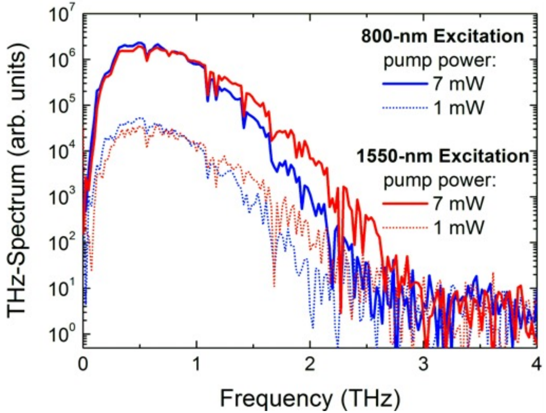

Papaioannou et al., Arxiv:1803.08838 (2018)

800-nm and 1550-nm excitation

Comparison with a 5-µm dipole LT-GaAs-based PCA emitter at 7 mW average excitation power:

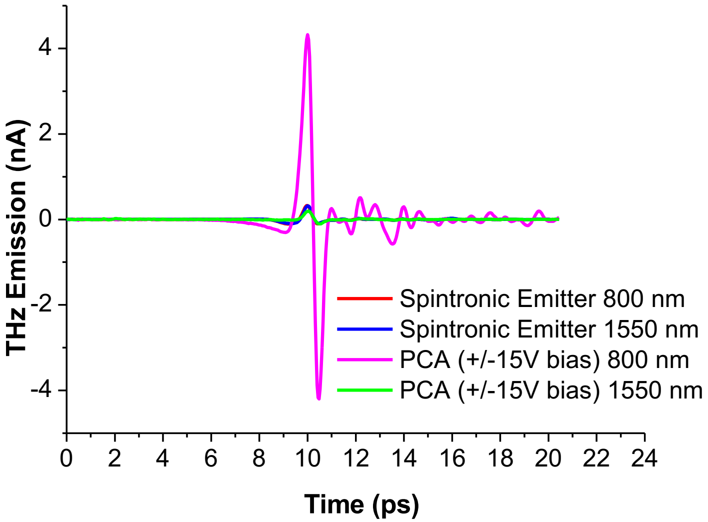

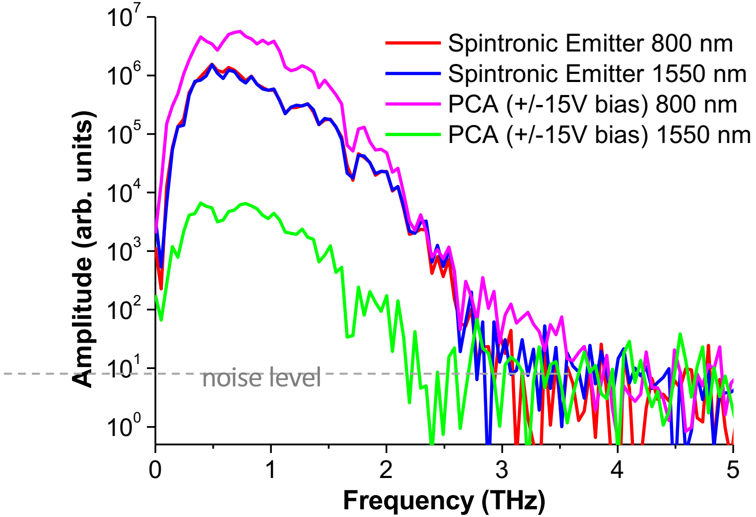

800-nm excitation: dipole PCA with best THz emission efficiency

1550-nm excitation: spintronic emitter with highest efficiency

High average power spintronic THz Emission

Large area STEs can be fabricated

High power/energy pump sources

Pump fluences up to 5 mJ/cm^2

THz field strengths up to 300 kV/cm

THz average powers up to several µW

Cooling of the substrate required

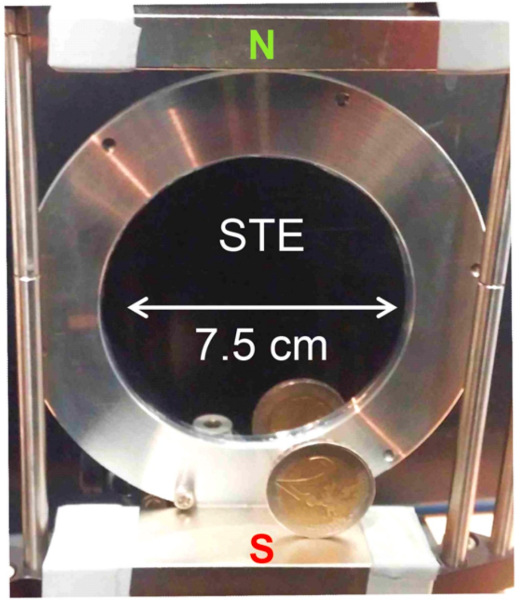

T. Vogel, et al., Optics Express **30,** pp. 20451-20468 (2022)

High average power spintronic THz Emission

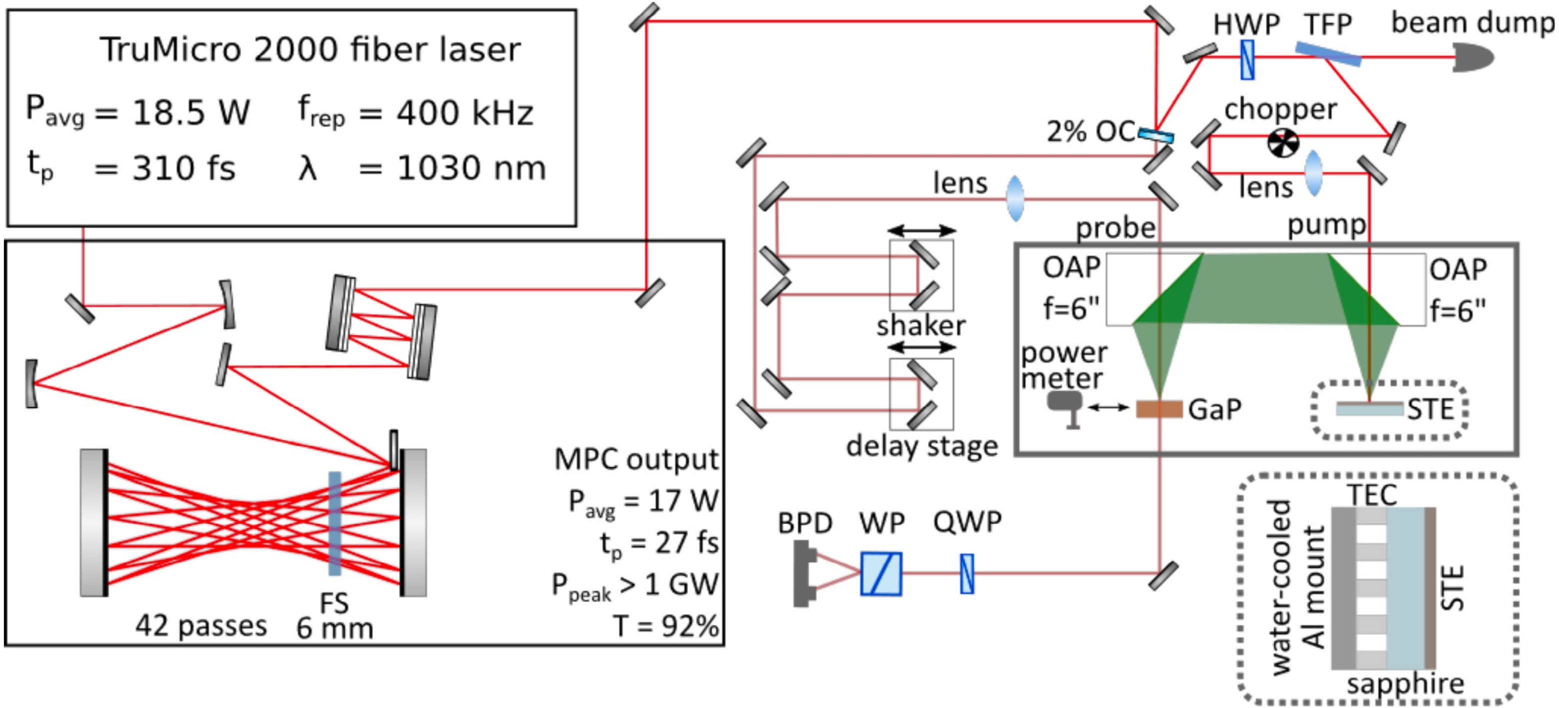

Tuesday, February 7th , 9:00 h, Clara Saraceno: „Ultrafast lasers for THz generation“

T. Vogel, et al., Optics Express **30**, pp. 20451-20468 (2022)

High average power spintronic THz Emission

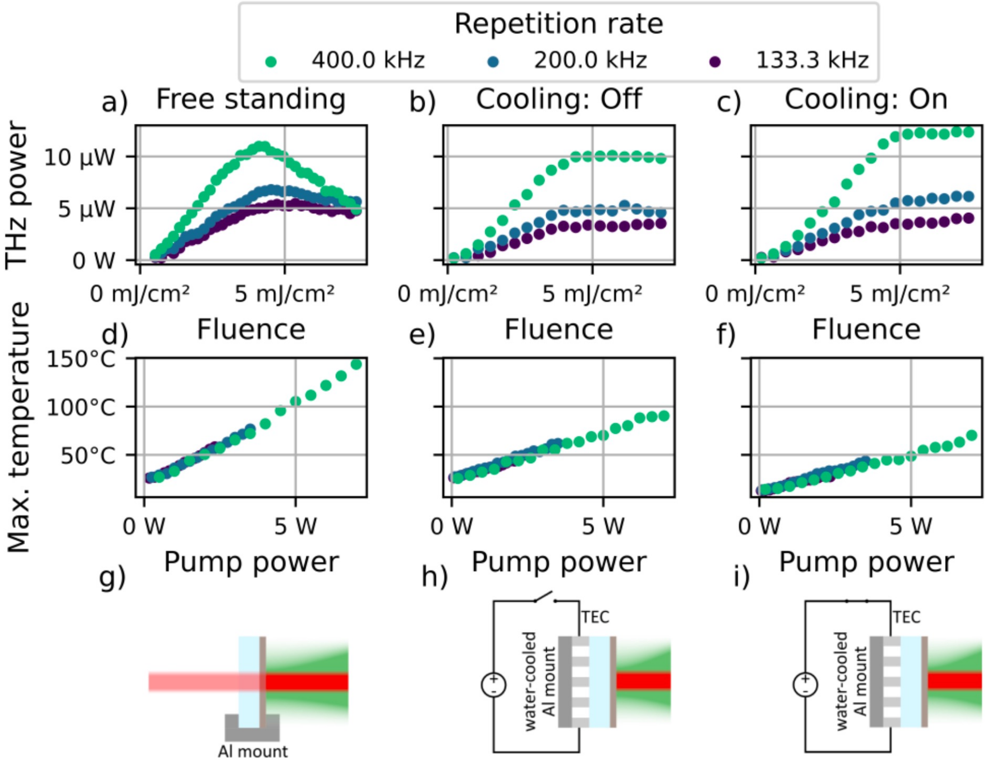

Efficient cooling required

Setup in reflection geometry

Large area emitter

T. Vogel, et al., Optics Express **30,** pp. 20451-20468 (2022)

Efficient spintronic terahertz emitters:
Basic principles and technical realization

RPTU

Content

- Introduction
- Femtosecond laser driven THz sources
- Spintronics and THz emission
- Technical realization
- Optimization and typical Results
- Outlook and Summary

Roadmap for Spintronic THz Emitters

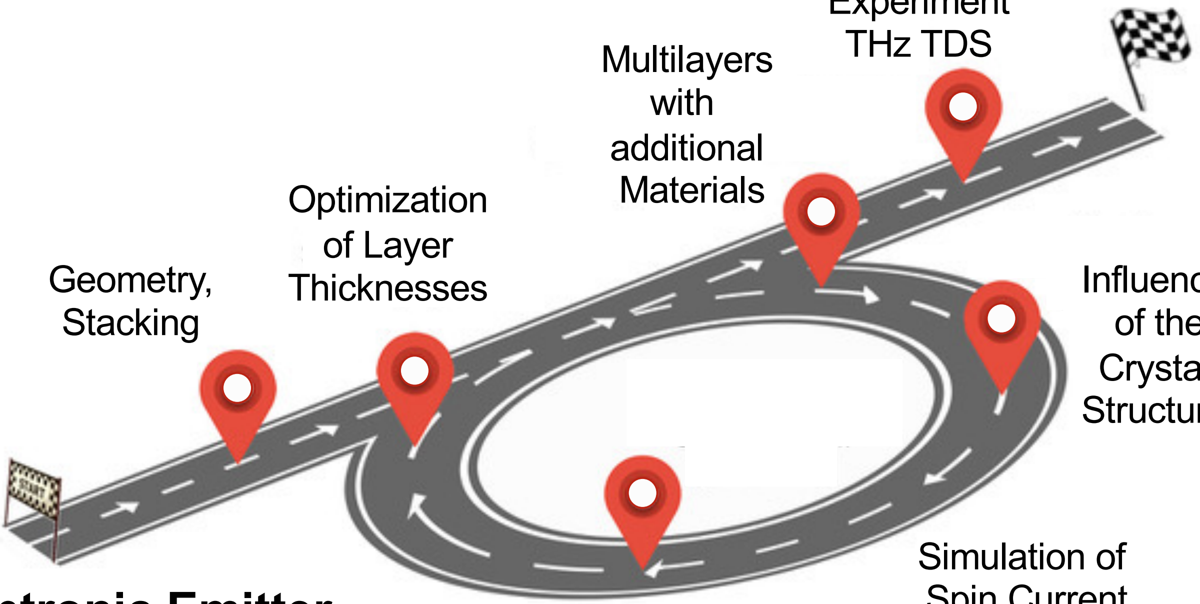

Experiment
THz TDS

Multilayers
with
additional
Materials

**Optimized Spintronic
THz Emitter**

Optimization
of Layer
Thicknesses

Geometry,
Stacking

Influence
of the
Crystal
Structure

Simulation of
Spin Current

Electrical & Optical
Properties

**Spintronic Emitter
Concept**

T. Seifert, Nat. Photon. **10**, 483 (2016)

Summary

Spintronic emitters are promising devices for THz TDS systems:

1. THz emission between 0.1 and 30 THz depending on pump pulse length and THz detector
2. STEs can be drive by virtually any pump wavelength
3. “High” efficiency and long term stability
4. Well established fabrication process
5. Linear pump fluence dependence up to 5 mJ/cm^2

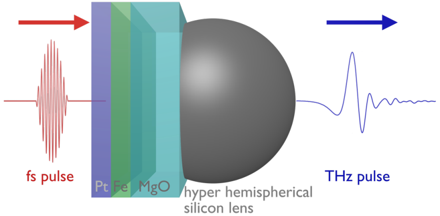

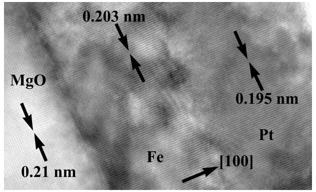

Summary

Spintronic emitters are promising devices for THz TDS systems:

6. Growth of large area STEs
7. Linearly polarized THz emission
8. Controlling the polarization by external magnetic field
9. STE thin films can easily be micro structured
10. No phase matching required due to thin film

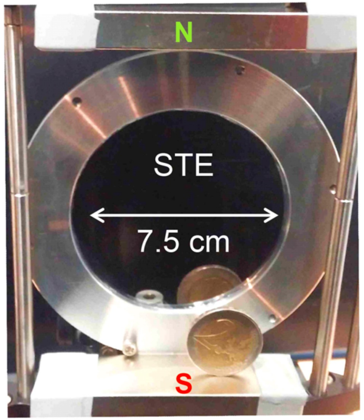

Outlook

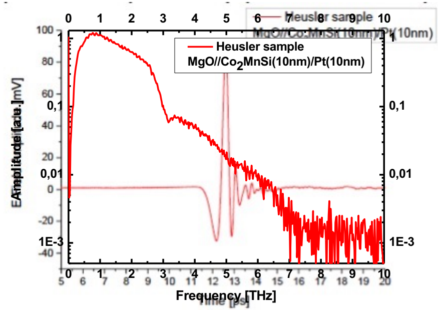

Investigation of new material systems (e.g. Heusler metals, antiferro- magnets, etc.)

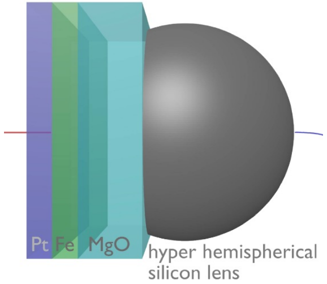

Improved emitter design (additional layers)

New substrates (HR-Si)

Use of different pump sources (1.5 µm)